



Staphylococcus epidermidis WF2R11 Suppresses PM_{2.5}-Mediated Activation of the Aryl Hydrocarbon Receptor in HaCaT Keratinocytes

Eulgi Lee¹ · Hyeok Ahn¹ · Shinyoung Park² · Gihyeon Kim¹ · Hyun Kim¹ · Myung-Giun Noh¹ · Yunjae Kim¹ · Jae-sung Yeon² · Hansoo Park^{1,2}

Accepted: 21 January 2022 / Published online: 21 June 2022
© The Author(s) 2022

Abstract

The skin supports a diverse microbiome whose imbalance is related to skin inflammation and diseases. Exposure to fine particulate matter (PM_{2.5}), a major air pollutant, can adversely affect the skin microbiota equilibrium. In this study, the effect and mechanism of PM_{2.5} exposure in HaCaT keratinocytes were investigated. PM_{2.5} stimulated the aryl hydrocarbon receptor (AhR) to produce reactive oxygen species (ROS) in HaCaT cells, leading to mitochondrial dysfunction and intrinsic mitochondrial apoptosis. We observed that the culture medium derived from a particular skin microbe, *Staphylococcus epidermidis* WF2R11, remarkably reduced oxidative stress in HaCaT cells caused by PM_{2.5}-mediated activation of the AhR pathway. *Staphylococcus epidermidis* WF2R11 also exhibited inhibition of ROS-induced inflammatory cytokine secretion. Herein, we demonstrated that *S. epidermidis* WF2R11 could act as a suppressor of AhRs, affect cell proliferation, and inhibit apoptosis. Our results highlight the importance of the clinical application of skin microbiome interventions in the treatment of inflammatory skin diseases.

Keywords Particulate matter · Keratinocyte · Aryl hydrocarbon receptor · *Staphylococcus epidermidis* · Skin microbiome

Introduction

Air pollution from particulate matter (PM) has detrimental effects on humans and animals [1]. Industries, cars, coal-fired power plants, and other anthropogenic activities contribute to air pollution, adversely affecting the environment and human health [2]. The US Environmental Protection Agency (EPA) classified PM according to particle size as PM_{0.1} (ultrafine, ≤ 0.1 μm), PM_{2.5} (fine, ≤ 2.5 μm), and PM₁₀ (coarse, ≤ 10 μm) [3]. PM_{0.1} and PM_{2.5} are the most prevalent among all types of PM. The adhesion of contaminants, oxidizing gases, organic compounds, or transition metals to PM_{0.1} and PM_{2.5} introduces toxins to the body [4, 5].

The skin, the largest organ of the human body, is a multi-layered structure comprising the epidermis, dermis, and

subcutaneous tissues [6, 7]. It is the primary barrier against external contaminants and serves as a repository for millions of microorganisms [8]. The composition of the skin microbial community depends upon the site and the presence of external irritants [9]. For instance, differences in fatty acid concentrations in the composition of a specific skin site cause changes in the abundance of bacterial species [10–13]. In a lipophilic environment, *Propionibacterium* species dominate, whereas, in moist areas, *Staphylococcus* and *Corynebacterium* species dominate. An imbalance in the composition of bacterial species—i.e., dysbiosis—destroys the diversity of the microbial community, causing deterioration and inflammation of the skin and a plethora of skin disorders [12, 14–16]. Airborne PM_{2.5} can cause severe skin diseases, including eczema, upon permeating the human skin cells [17]. However, alterations in skin microbiomes as a result of PM_{2.5}-induced dermatitis have not been evaluated.

PAHs contained in PM_{2.5} mediate many biological effects, including carcinogenicity and developmental defects [18–20]. Several PAHs are direct activators of the aryl hydrocarbon receptor (AhR) and may subsequently play a crucial role in the induction and action of cytochrome P450 (CYP) 1A1 and 1B1 [19, 21]. Most PAHs are not

✉ Hansoo Park
hspark27@gist.ac.kr

¹ Department of Biomedical Science and Engineering, Gwangju Institute of Science and Technology (GIST), Gwangju 61005, Republic of Korea

² Genome and Company, Pangyo-ro 253, Bundang-gu, Seoungnam-si, Gyeonggi-do 13486, Republic of Korea

water-soluble, but substances such as anthracene, benz[a]anthracene, and benzo[a]pyrene are capable of secondary oxidation to water-soluble oxygen metabolites (oxy-PAH) [22–24]. These PAHs can act as potent regulators of CYP1 family enzymes and trigger the activation of AhR and sub-mechanisms (Table 1) [25]. Therefore, *CYP1* and *Cox-2* are deemed important functional biomarkers involved in AhR-mediated signaling. In addition to the PAHs constituting PM_{2.5}, PM_{2.5} comprises various transition metals and organic compounds, which can induce excessive ROS production in mitochondria and cell cytoplasm [26]. It induces oxidative stress directly in the epidermis and dermis, triggers inflammation, and affects cell proliferation and apoptosis [27].

Simultaneously, increased free radical production in skin tissue stimulates the release of inflammatory cytokines, such as tumor necrosis factor-alpha (TNF- α) and interleukins (ILs). These cytokines induce activated neutrophil infiltration and phagocytic production of radicals [28, 29]. Excessive accumulation of ROS triggers apoptosis through *Cox-2* and TNF- α . Nuclear factor-kappa B (NF- κ B) translocation to the nucleus induces apoptosis by downregulating Bcl-2,

upregulating Bax, releasing cytochrome-c from mitochondria, and activating caspases [30–32]. We investigated whether *Staphylococcus epidermidis* WF2R11, a member of the human skin microbiome, alleviates the oxidative stress generated due to PM_{2.5}-mediated ROS accumulation, and whether *S. epidermidis* WF2R11 inhibits PM_{2.5}-induced apoptosis in human skin keratinocytes (HaCaT) in vitro.

Methods

AhR Complex Gene Set Score Analysis of Gene Expression Data from Public Resources

All processed gene expression data used in this study were procured from the Gene Expression Omnibus repository with accession number GSE107871 [30]. This RNA-seq dataset contained 24 samples, which consisted of the lesion site of a psoriasis patient, non-lesion area of the psoriasis patient, and skin from normal control groups [30]. The processes of patient recruitment, sampling, and RNA sequencing have been previously described by Mohan [30]. To

Table 1 Certified mass fraction values for PAHs in urban particulate SRM 1648a

PAHs	Mass fraction (mg/kg)	Water-soluble (at 25 °C)	AhR regulation	CYP regulation
Phenanthrene	4.86 ± 0.17	Soluble (1.15 mg/L)	Activation	Activation
2-Methylphenanthrene	0.96 ± 0.12	Insoluble		
3-Methylphenanthrene	0.614 ± 0.067	Insoluble		
Fluoranthene	8.07 ± 0.14	Soluble (265 µg/L)	Activation	Inhibition
Pyrene	5.88 ± 0.07	Insoluble		
Benzo[g,h,i]fluoranthene	1.17 ± 0.05	Insoluble		
Benz[a]anthracene	2.71 ± 0.15	Insoluble		
Chrysene	6.12 ± 0.06	Insoluble		
Triphenylene	2.04 ± 0.13	Soluble (6.6 µg/L)		
Benzo[k]fluoranthene	3.03 ± 0.24	Insoluble		
Benzo[e]pyrene	4.85 ± 0.07	Soluble (0.2 to 6.2 µg/L)		
Benzo[a]pyrene	2.57 ± 0.10	Soluble (0.2 to 6.2 µg/L)	Activation	Activation
Perylene	0.742 ± 0.048	Nearly insoluble		
Benzo[g,h,i]perylene	5.00 ± 0.18	Insoluble		
Indeno[1,2,3,-cd]pyrene	4.17 ± 0.17	Insoluble		
Dibenz[a,j]anthracene	0.407 ± 0.039	Soluble (0.00166 mg/L)	Activation	Activation
Benzo[b]chrysene	0.405 ± 0.041	Insoluble		
Picene	0.586 ± 0.058	Insoluble		
Coronene	2.28 ± 0.10	Soluble (0.14 µg/L)	Activation	Activation
Dibenzo[b,k]fluoranthene	0.947 ± 0.054	Insoluble		
Dibenzo[a,e]pyrene	0.622 ± 0.045	Insoluble		

calculate the AhR score, gene set variation analysis (GSVA) was performed using the AhR complex gene set of harmonizome databases using the GSVA package in R Project 4.2.0 program [33]. In the GSVA package, the “ssgsea” method was used, and the analysis was carried out between a minimum size of 10 and a maximum size of 500 [34].

Human Skin Sample Collection and Preparation

The study for the isolation of permanent bacteria on the skin was approved by the Institutional Review Board (IRB; P01-201,605–31-003) of Korea National Institute for Bioethics Policy (KONIBP). All study protocols adhered to relevant ethical guidelines. In addition, all participants provided written informed consent before enrolment. In addition, this study protocols adhered to relevant ethical guidelines and regulations. Skin samples were collected from donors who had no history of skin disease. Before collecting the skin samples, the participants were asked not to wash their faces for longer than 12 h. Samples were obtained by rubbing the donor’s face for 1 min or 20 times vigorously with a sterilized cotton swab soaked in distilled water and were then placed in a 10-mL trophic soy broth (TSB) solution.

Microbial Sample Isolation and 16S rRNA PCR Amplification and Sequencing

The skin samples collected from ten donors were diluted to 10^{-1} – $10^{-\text{threefold}}$ using phosphate-buffered saline (PBS). Then, 100 μL of each diluted solution was spread onto R2A, TSB, Luria–Bertani, MRS (De Man, Rogosa, and Sharpe), and blood (Columbia agar with 5% sheep blood) agar plates (Bio-Rad, Hercules, CA, USA). The inoculated plates were incubated at 37 °C for up to 72 h; whereafter, the single colonies on the plates were picked up, and their 16S rRNA genes were amplified using colony PCR. The applied parameters for the PCR were as follows: initial denaturation at 95 °C for 15 min, then 32 cycles of denaturation at 95 °C for 30 s, annealing at 55 °C for 30 s, and extension at 72 °C for 1 min and 45 s, and then a final extension step at 72 °C for 5 min. The primers for PCR were 27F (5′-AGAGTTTGATCCTGGCTCAG-3′) and 1492R (5′-GGTACCTTGTTACGACTT-3′). Purification of the amplified DNA was carried out using the EZ-pure PCR Purification Kit (Ver 2, Enzymomics, Daejeon, South Korea), and the nucleotide sequences of the genes were determined using the ABI 3730xl system (Macrogen, Seoul, South Korea). For phylogenetic analysis, the 16S rRNA gene sequences were analyzed using the nucleotide BLAST program available at the NCBI website (https://blast.ncbi.nlm.nih.gov/Blast.cgi?PROGRAM=blastn&PAGE_TYPE=BlastSearch&LINK_LOC=blasthome).

Hemolysis Tests for Isolated Bacteria

For hemolysis testing of the isolated bacteria, 73 single colonies were obtained by streaking bacterial samples onto TSB plates using an inoculation loop. The colonies were re-streaked onto blood agar plates (trypticase soy agar with 5% sheep blood) and incubated at 37 °C. The color of the colonies, indicating the hemolysis pattern, was noted at 48 h. From the isolation and subsequent analysis of 16S rRNA gene sequences, 50 species and 135 strains, including a variety of skin bacteria, were identified (data not shown). Hemolysis analysis of the isolated bacteria showed that most of the microbes had a β (35 strains) or γ pattern (37 strains), and the α pattern (1 strain) was not frequently observed (data not shown). For further analyses, six strains that showed γ (gamma) hemolysis patterns were selected.

Preparation of PM_{2.5}

Urban PM NIST 1648a (PM_{2.5}) was purchased from Sigma-Aldrich, St. Louis, MO, USA. The PM_{2.5} dose used in this study was established based on US EPA air quality standards for particulate pollution and AQI (Air Quality Index) revisions. The composition and AQI category of Urban PM NIST 1648a are indicated in Table 1. PM_{2.5} stock solutions (50, 100, and 200 $\mu\text{g}/\text{mL}$) were prepared in DMEM and sonicated for 10 min to avoid agglomeration of the suspended PM_{2.5} particles. All experiments were performed within 1 h of stock preparation to avoid variability in PM_{2.5} compositions in the solution.

Cell Culture and Treatment of PM_{2.5} with Se Solution

HaCaT cells were purchased from PromoCell (Heidelberg, Germany). A total of 3×10^5 HaCaT cells were maintained at 37 °C in an incubator with a humidified atmosphere of 5% CO₂ and are tested four times per year for mycoplasma using PCR. All studies were conducted within 6 months of the latest test date (11–2020). HaCaT cells were cultured in DMEM with 10% heat-inactivated FBS and an antibiotic–antimycotic (100 units/mL penicillin, 100 $\mu\text{g}/\text{mL}$ streptomycin, and 0.25 $\mu\text{g}/\text{mL}$ amphotericin B) (Gibco, Thermo Fisher Scientific, Waltham, MA, USA) for no longer than 4 weeks before use. For PM_{2.5} treatment, HaCaT cells were inoculated in 6-well plates, incubated in an atmosphere of 5% CO₂ at 37 °C, and grown till they achieved 80% confluence. After 12 h, the cells were washed once with PBS, and 2 mL of each concentration of PM_{2.5} stock solution was added to the cells, depending on the purpose of the in vitro assays. Then, 10% of conditioned *S. epidermidis* WF2R11 medium (i.e., Se solution) was added to the cells together with a supplement-free medium simultaneously as PM_{2.5} treatment.

AhR, CYP1A1 Gene Knockdown

siRNA against human *AhR* and *CYP1A1* mRNA was commercially synthesized by Bioneer, Daejeon, South Korea: siAHR (forward, 5'-CACUCAGACUACCACACAU-3', reverse, 5'-AUGUGUGGUAGUCUGAGUG-3'); siCYP1A1 (forward, 5'-GCUAGGGUUAGGAGGUCCU-3', reverse, 5'-AGGACCUCCUAACCCUAGC-3'). To transfect the siRNA oligo, we used Lipofectamine™ RNAiMAX (Invitrogen, Carlsbad, CA, USA) according to the manufacturer's instructions. Briefly, 24 h before transfection, 3×10^5 HaCaT cells were seeded onto 6-well plates with 2.5 mL of growth medium without antibiotics to reach 50–60% confluence at the time of transfection. AhR and CYP1A1 siRNA were incubated with HaCaT cells for 24 h. The efficiency of gene silencing by siRNA was evaluated using real-time PCR (qPCR).

Cell Viability Assay

HaCaT cells (3×10^5) were seeded into 48-well plates and incubated for 24 h in 2 mL of the complete medium. Then, 1, 5, 10, 20, or 30% of *S. epidermidis* WF2R11 culture supernatant was added to the cells, respectively, and incubated for another 48 h. After washing the cells once with PBS, 3-(4,5-dimethylthiazol-2-yl)-2,5-diphenyltetrazolium bromide (MTT) solution was added to each well, and the plates were incubated for 4 h. Then, the medium was discarded, and dimethyl sulfoxide was added to dissolve the formazan crystals. Optical density was measured at 570 nm using a microplate reader and was normalized relative to the untreated control.

RNA Isolation and qPCR

Total RNA was isolated from cells using TRIzol reagent (TaKaRa, Shiga, Japan) according to the manufacturer's instructions. cDNA was synthesized from 1 µg total RNA using the Reverse Transcription Premix (Elpis-Biotech, Daejeon, South Korea) under the following reaction conditions: 45 °C for 45 min and 95 °C for 5 min. Gene expression was quantified using qPCR, and data were analyzed using the StepOne Plus™ software (Applied Biosystems, Foster City, CA, USA). qPCR amplification reactions were performed using SYBR Green PCR Master Mix with premixed ROX (Applied Biosystems, Foster City, CA, USA). The following primer pairs (Bioneer, Daejeon, South Korea) were used in the ABI 7300 Cyclor internal reaction according to the manufacturer's protocol (Online Resource 7). The reaction conditions were as follows: 40 cycles for

2 min at 50 °C, 10 min at 95 °C, 10 s at 95 °C, and 1 min at 60 °C. 18S rRNA was used as an internal control.

Measurement of Proinflammatory Cytokine Concentrations

The proinflammatory cytokines (IL-1β, IL-6, IL-8, and IFN-γ) produced were measured using an ELISA assay. HaCaT cells (6×10^5), seeded in 6-well culture plates, were pretreated with PM_{2.5} (50, 100, and 200 µg/mL) for 12 h and then treated with the supernatant of the *S. epidermidis* WF2R11 for 12 h. After the treatment period, aliquots of samples (100 µL/well) were collected from the experimental medium, and the production of cytokines (IL-1β, IL-6, IL-8, and IFN-γ) was measured using a Human ILs Quantikine ELISA Kit (R&D Systems, Minneapolis, MN, USA) according to the manufacturer's instructions.

Western Blotting for Measuring Protein Expression

Total HaCaT cells protein was extracted using lysis buffer (Thermo Fisher Scientific, Waltham, MA, USA) supplemented with protease/phosphatase inhibitor cocktail on ice for 30 min. BCA kit was used to measure the concentration of the proteins and for protein quantification. Proteins (20 µg) were mixed with loading buffer, separated using 10% sodium dodecyl sulfate–polyacrylamide gel electrophoresis (SDS-PAGE), and transferred to polyvinylidene fluoride (PVDF) membranes (Bio-Rad, Hercules, CA, USA). The PVDF membranes were blocked with 5% skim milk in Tris-buffered saline with Tween (TBST) for 2 h at 37 °C and incubated with primary antibodies against β-actin (1:2000), Bax (1:1000 dilution), Bcl-2 (1:500 dilution), p38 (1:1000 dilution), p-p38 (1:1000 dilution), JNK (1:1000 dilution), p-JNK (1:1000 dilution), ERK (1:2000 dilution), and p-ERK (1:2000 dilution) at 4 °C overnight. After washing 3 times with TBST, PVDF membranes were incubated with appropriate secondary antibodies for 1 h at room temperature. The immunoblots were visualized with a chemiluminescence detection system. The optical density (OD) of western blot bands was measured using ImageJ software (National Institute of Health, Bethesda, MD, USA). The data was normalized to the level of reference proteins and then averaged and presented as a relative fold change of control, from at least three independent experiments.

Annexin V-PI Assay for Mitochondrial Apoptosis

For Annexin V-Pi assays, HaCaT cells were stained with Annexin V-FITC and PI and assessed for mitochondrial apoptosis using flow cytometry according to the

manufacturer's protocol (Sigma-Aldrich, St. Louis, MO, USA). Early apoptotic cells (annexin V positive, PI negative), necrotic cells (annexin V positive, PI positive), and viable cells (annexin V negative, PI negative) were classified using flow cytometry and fluorescence detection of annexin V bound to HaCaT cells. Apoptotic cells were filtered and determined using flow cytometry (BD FACS Calibur, Franklin Lakes, NJ, USA). The data processing was performed using the FlowJo 7.6.1 software.

Mitochondrial Superoxide Detection

For the measurement of mitochondrial peroxide, HaCaT cells treated with different concentrations of PM_{2.5} were detected with fluorescence microscopy using MitoSOX™ Red Mitochondrial Superoxide indicator (Thermo Fisher, St. Louis, MO, USA) as a specific fluorescence probe. HaCaT cells treated with PM_{2.5} were incubated with 5 μM of the probe for 30 min at 37 °C in the dark. Then, cells were thoroughly washed with warm Hank's balanced salt solution (HBSS) buffer and mounted for imaging. MitoSOX™ Red-stained cells were visualized at an excitation wavelength of 510 nm and an emission wavelength of 580 nm.

Mitochondrial Membrane Potential ($\Delta\psi_m$) Measurement

The mitochondrial membrane potential and early stage of apoptosis were analyzed via fluorescence microscopy after staining with 5,5,6,6-tetrachloro-1,1,3,3-tetraethylbenzimidazolylcarbocyanine iodide (JC-1, Invitrogen, Carlsbad, CA, USA), a lipophilic cationic fluorescence dye. JC-1 dye is characterized by green fluorescence emission at ~529 nm in the monomeric form of the probe, which changes to red (~590 nm) with the concentration-dependent formation of red J-aggregates.

Diff-Quik Staining for Observing Cytological Features

Diff-quick (catalog no. 111661; Merck, Darmstadt, Germany) staining preparations of HaCaT cells were obtained by spreading 3×10^5 normal cells onto LAB-TEK® chamber slides (Thermo Fisher, St. Louis, MO, USA), treating the cells with 100 μg/mL PM_{2.5}, and incubating the slides for 24 h at 37 °C. A thin smear of each HaCaT was stained using the diff-quick staining by manufacturer's instructions. Briefly, the air-dried smears were sequentially dipped five times in a methanol fixative solution I, five more times in stain solution II (color reagent red), then dipped five times in stain solution III (color reagent blue), and gently rinsed with distilled water. The overall staining process took ~40 s. The

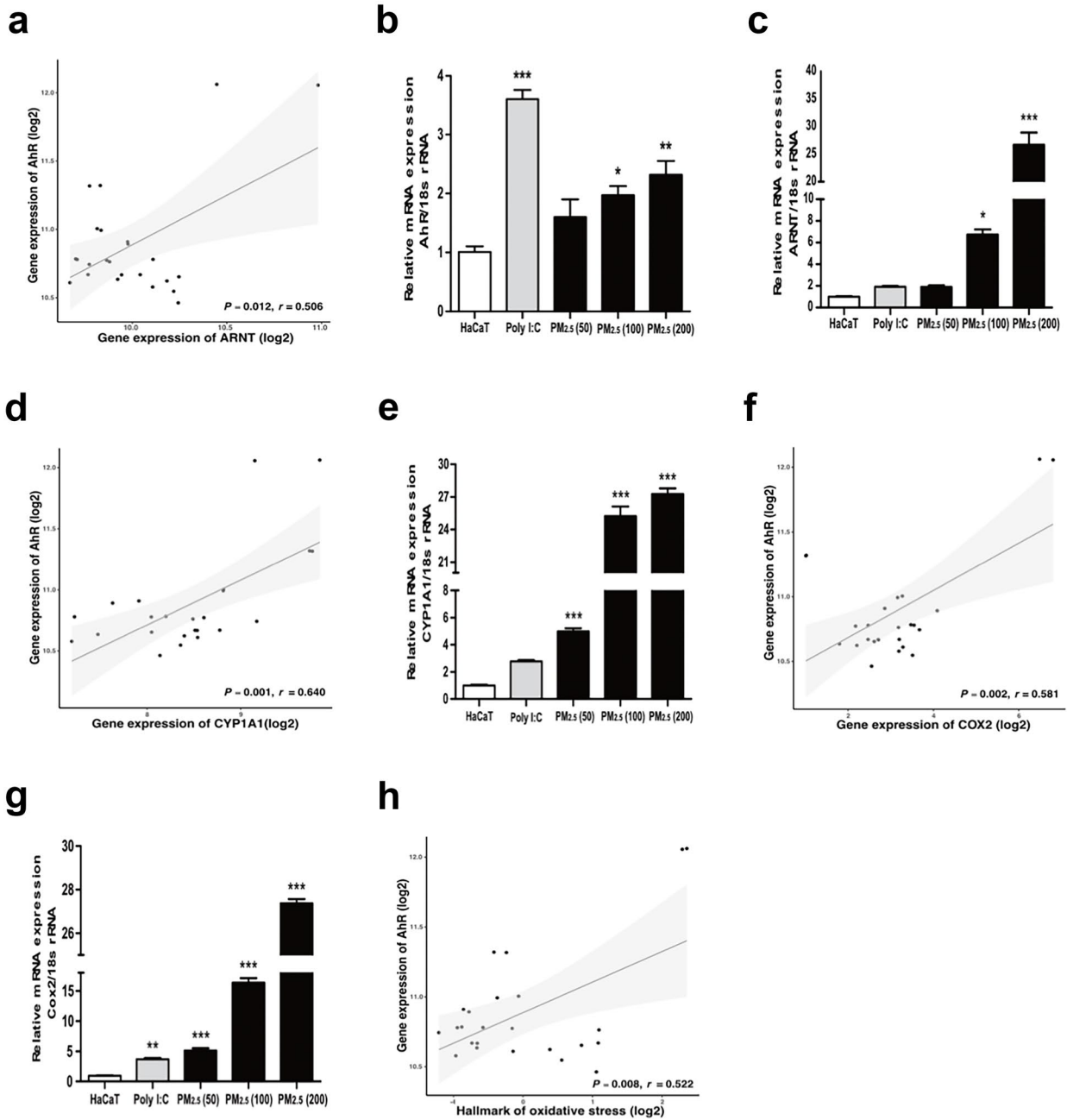
slides were then cleared in xylol and mounted in a non-aqueous mounting medium. A diff-quick-stained smear of each HaCaT slide was analyzed by a board-certified pathologist (MGN).

Ki-67 Immunohistochemistry

HaCaT cells were prepared by spreading 3×10^5 normal cells onto LAB-TEK® chamber slides (Thermo Fisher, St. Louis, MO, USA), followed by treatment with 100 μg/mL PM_{2.5}, and incubation for 24 h at 37 °C. After removing the chamber wall, all the slides were fixed in neutral-buffered formalin. Endogenous peroxidase activity was blocked by incubating with 3% hydrogen peroxidase in methanol for 5 min. Epitope retrieval of Ki-67 was carried out by boiling in a pressure cooker in Tris–EDTA solution buffer at pH 9.0 for 15 min at 99 °C. After washing with PBS, the sections were incubated with the anti-human Ki-67 polyclonal antibody (ab15580, rabbit anti-human; Abcam, Cambridge, MA, USA) at a dilution of 1:600 using an antibody diluent (GBI Labs, Bothell, WA, USA) for 60 min at 23–25.5 °C. The primary antibody against Ki-67 was detected with Polink-2 Plus HRP Rabbit with DAB Kit (GBI Labs, Bothell, WA, USA) for 30 min at approximately 23–25.5 °C. Diaminobenzidine (Sigma-Aldrich, St. Louis, MO, USA) was used as the chromogen and incubated for 3 min at 25 °C. The slides were counterstained with hematoxylin. For the positive control, a normal tonsil tissue was used; for the negative control, the primary antibody was omitted, and PBS was used in each experiment. The Ki-67 index was quantified by estimating the number of positive HaCaT cells expressing nuclear Ki-67 (brown colored) among the total number of HaCaT cells. Both weakly and strongly labeled nuclei were included in the estimates of proliferating cells. All immunostained slides were evaluated twice by a blinded board-certified pathologist (MGN). A semi-quantitative assessment of the average percentage of Ki-67 positive cells in several fields comprising more than 1000 cells was performed.

Statistical Analysis

All data were tested for normality, and the dataset was analyzed using one-way ANOVA. The post hoc analysis was then carried out using the Bonferroni test for comparison between pairs. All results are presented as the mean ± SEM. Correlations were determined using Pearson's correlation analysis. All statistical analyses were performed using GraphPad Prism 5.02 (GraphPad Software, San Diego, CA, USA) and R-4.2.0 for Windows. The statistical significance was set at $p < 0.05$.



i

Mito-sox staining

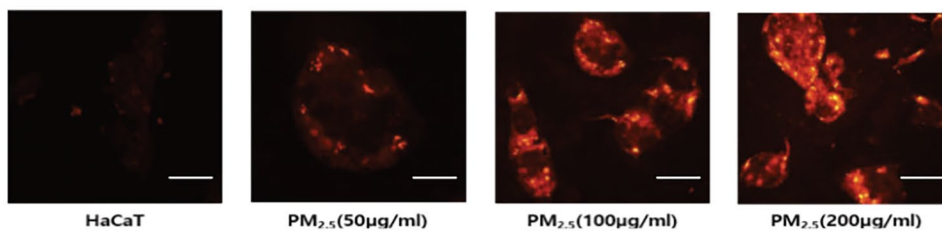


Fig. 1 PM_{2.5} activates the AhR signaling pathway, leading to ROS production. (a) Correlation analysis of AhR with ARNT expression reveals their positive correlation at the mRNA level. (b) Measurement of the mRNA level of *AhR* relative to 18S rRNA. (c) Measurement of the mRNA level of *ARNT* relative to 18S rRNA. (d) Correlation analysis of *AhR* with *CYP1A1* expression reveals their positive correlation at the mRNA level. (e) Measurement of the mRNA level of *CYP1A1* relative to 18S rRNA. (f) Correlation analysis of *AhR* with *Cox-2* expression reveals their positive correlation at the mRNA level. (g) Measurement of the mRNA level of *Cox-2* relative to 18S rRNA. (h) Correlation analysis of AhR with the hallmark of oxidative stress reveals their positive correlation at the mRNA level. (i) Measurement of Mito-SOX fluorescence expression when treated with 50, 100, and 200 µg/mL of PM_{2.5} compared to that of the control HaCaT cells. Scale bar, 20 µm. The mRNA level of *AhR*, *ARNT*, *CYP1A1*, and *Cox-2* relative to 18S rRNA was measured after 12 h of PM_{2.5} treatment for each concentration. Correlation was determined using Pearson's correlation analysis. Bonferroni test for comparison between pairs was used to calculate statistical significance. * $p < 0.05$, ** $p < 0.01$, *** $p < 0.001$, or ns, non-significant; compared to normal HaCaT cells. AhR, aryl hydrocarbon receptor; ARNT, AhR nuclear translocator

Results

PM_{2.5} Stimulates AhR to Induce ROS Production in HaCaT Cells

AhR signaling is associated with exposure to PM_{2.5} and ROS production [35]. To reaffirm the relationship between PM_{2.5}, AhR stimulation, and ROS production, we performed RNA-seq analysis of whole skin using open-access data from a study by Swindell [36]. The transcriptomic analysis involved in the AhR signaling pathway were identified to predict the association between the AhR-related genes and ROS production. We first analyzed the correlation between AhR and AhR nuclear translocator (ARNT) upon exposure to PM_{2.5}. *AhR* expression was positively correlated with *ARNT* expression ($p = 0.012$, $r = 0.506$) (Fig. 1a). To prove the positive correlation of AhR-ARNT gene expression evidenced by transcriptomic analysis, after PM_{2.5} treatment in HaCaT cells, mRNA expression levels of both genes were measured. The dosage of PM_{2.5} classified each concentration of PM_{2.5} in accordance with EPA standards (Online Resource 1). Each concentration of PM_{2.5} used in the following experiments was set to moderate (PM_{2.5}; 50 µg/mL), unhealthy (PM_{2.5}; 100 µg/mL), hazardous (PM_{2.5}; 200 µg/mL). Similar to the correlation between the two genes presented in Fig. 1a, AhR and ARNT mRNA expression significantly increased as the PM_{2.5} concentration increased, suggesting the possibility that PM_{2.5} may act as a ligand for AhR and induce the AhR/ARNT complex formation (Fig. 1b, c). As a sub-mechanism of the AhR/ARNT complex, *CYP1A1* and *Cox-2* play important roles in ROS production in the cytoplasm [37, 38]. The expression of *CYP1A1* positively correlated with *AhR*

expression ($p = 0.001$, $r = 0.640$; Fig. 1d). Furthermore, the expression of *Cox-2* positively correlated with that of *AhR* ($p = 0.002$, $r = 0.581$; Fig. 1f). The mRNA expression of each of these two genes increased from approximately fivefold to over 27-fold upon exposure to PM_{2.5} at minimal and maximal concentrations of 50 µg/mL and 200 µg/mL, respectively (Fig. 1e, g). PM_{2.5} reportedly upregulates ROS production and induces oxidative stress via AhR signaling ($p = 0.008$, $r = 0.522$; Fig. 1h) [37, 39]. To observe mitochondrial ROS accumulation, HaCaT cells were treated with varying concentrations of PM_{2.5}, and the ROS levels were observed using a Mito-SOX fluorescent dye that specifically targets mitochondria (Fig. 1i). The increase in red fluorescence is related to the oxidation of the MitoSOX Red reagent by peroxide in the mitochondria. Therefore, as the concentration of PM_{2.5} increased, ROS accumulation in the mitochondria was observed to increase substantially.

PM_{2.5} Induces Mitochondrial Dysfunction and Promotes Intrinsic Mitochondrial Apoptosis

Free radicals that have accumulated in the cytoplasm initiate oxidative damage mechanisms in various organelles, including mitochondria [31, 40]. Accumulation of cytoplasmic ROS in HaCaT cells causes mitochondrial dysfunction, increasing the expression of the mitochondrial apoptosis factor, *Bax*, and decreasing the expression of apoptosis inhibitor, *Bcl-2* [41, 42]. Thus, the increase in the ratio of *Bax/Bcl-2* via ROS is defined as a direct marker of mitochondrial damage. Using correlation analysis, *Bax* was positively correlated with the expression of *Cox-2* ($p < 0.001$, $r = 0.785$; Fig. 2a). After treatment with 100 µg/mL PM_{2.5}, the mRNA level of *Bax* was significantly increased compared to that of the control HaCaT cells and the positive control polyinosinic:polycytidylic acid (poly I:C group) (Fig. 2b). Meanwhile, the expression of *Bcl-2* showed significant negative correlation with *Cox-2* expression ($p < 0.001$, $r = 0.512$) in the transcriptomic analysis (Fig. 2c). The mRNA levels of *Bcl-2* also showed an inverse trend compared to that of *Bax*. Although not significant, the reduction in *Bcl-2* mRNA levels was remarkable compared to that of the control HaCaT cells (Fig. 2d). Also, the hallmark genes of oxidative stress induced by PM_{2.5} showed a significant positive correlation with the Kyoto Encyclopedia of Genes and Genomes (KEGG) category, apoptosis ($p < 0.001$, $r = 0.769$; Fig. 2e). Compared to the normal HaCaT cells and poly I:C-treated group, the PM_{2.5}-treated group was evaluated as a factor that significantly increased mitochondrial dysfunction (Fig. 2f). Furthermore, the intercellular density of the control HaCaT cells and the PM_{2.5}-treated cells (100 µg/mL) was compared and analyzed. Control HaCaT cells showed high intercellular density and evidence of persistent mitosis, whereas, in the

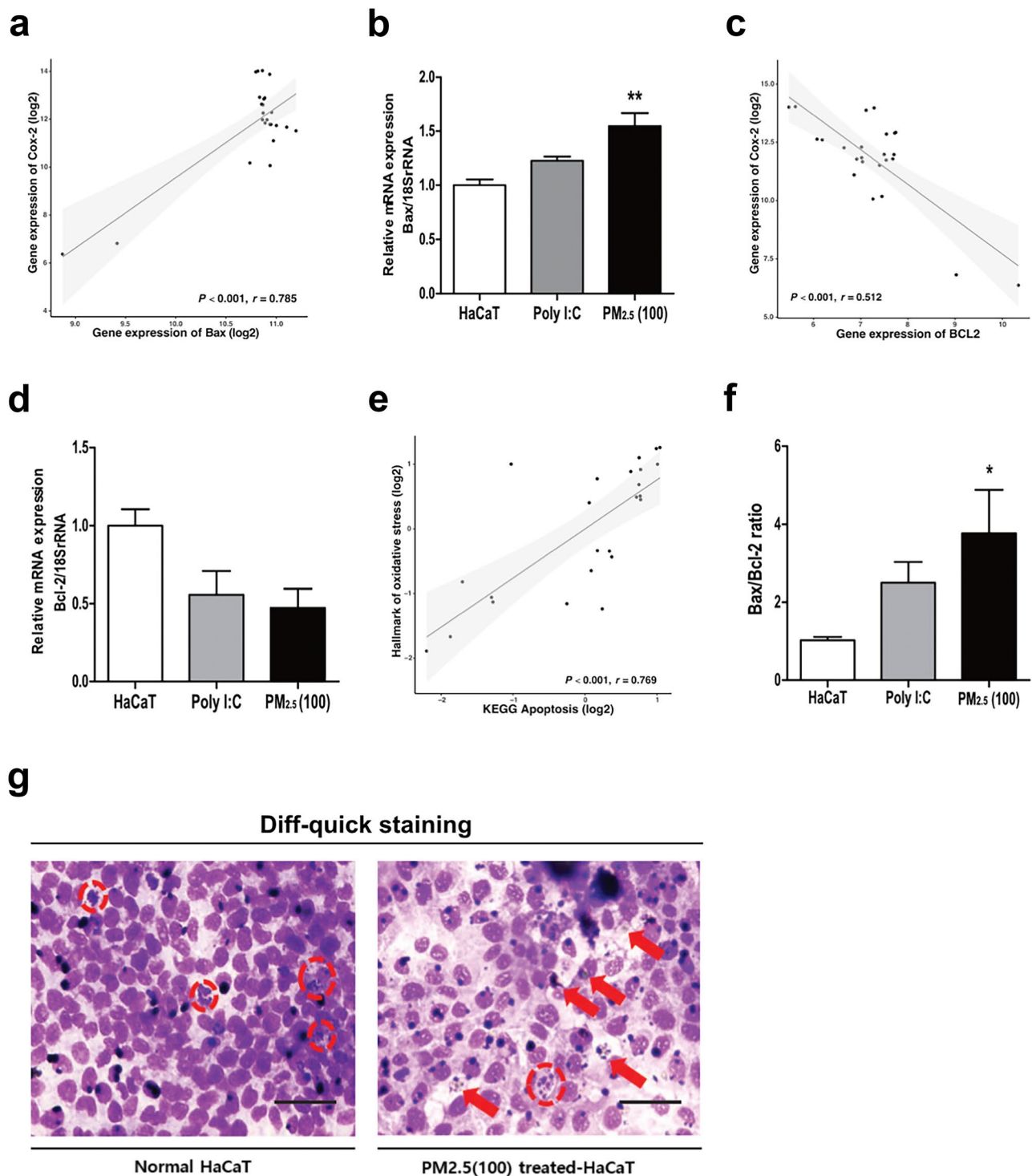


Fig. 2 Oxidative stress caused by ROS accumulation in the cytoplasm is closely related to apoptosis. (a) Correlation analysis of *Cox-2* with *Bax* expression reveals their positive correlation at the mRNA level. (b) Measurement of the mRNA level of *Bax* relative to 18S rRNA. (c) Correlation analysis of *Cox-2* with *Bcl-2* expression reveals their negative correlation at the mRNA level. (d) Measurement of the mRNA level of *Bcl-2* relative to 18S rRNA. (e) Correlation analysis of hallmark genes of oxidative stress with KEGG-apoptosis reveals their positive correlation. (f) Measurement of the relative *Bax*/*Bcl-2* ratio for mitochondrial-dependent cell death after PM_{2.5} treatment.

(g) Diff-quick staining for observing cytological features of 100 μg/mL PM_{2.5}-treated group compared to control HaCaT cells (normal HaCaT: red circle, mitosis progression; PM_{2.5}-treated-HaCaT: red arrows, nuclear degeneration; red circle, apoptosis). Scale bar, 50 μm. The mRNA level of *Bax* and *Bcl-2* relative to 18S rRNA was measured after 12 h of PM_{2.5} treatment for each concentration. Correlation was determined using Pearson's correlation analysis. Bonferroni test for comparison between pairs was used to calculate statistical significance. * $p < 0.05$, ** $p < 0.01$, *** $p < 0.001$, ns, non-significant; compared to normal HaCaT cells

PM_{2.5}-treated cells, the intercellular density was low, and indicators of nuclear degeneration as well as apoptosis were evident (Fig. 2g). As a result, an increased *Bax/Bcl-2* ratio in HaCaT cells may indicate the onset of intrinsic mitochondrial apoptosis upon exposure to PM_{2.5} [43].

***Staphylococcus epidermidis* WF2R11 Supernatant (Se Solution) Reduces the mRNA Levels of Inflammatory Cytokines Induced via PM_{2.5}**

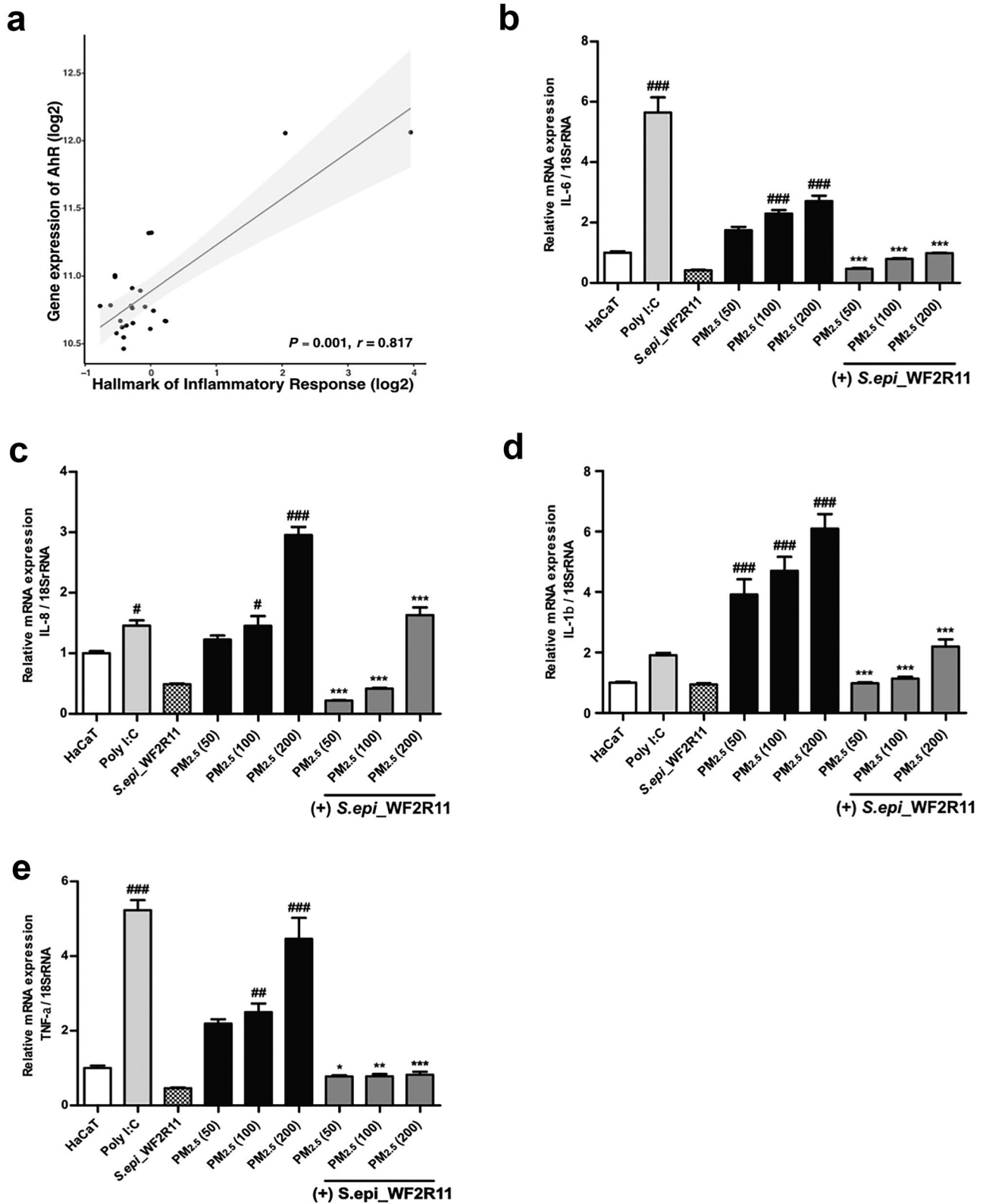
The AhR signaling pathway plays an important role in controlling the innate and adaptive immune response [44, 45]. The correlation between hallmark genes related to the immune response was analyzed according to the expression level of the *AhR* ($p < 0.001$, $r = 0.817$; Fig. 3a). AhR signaling is also closely related to the induction of oxidative stress, as shown in previous results. Similarly, an increase in oxidative stress led to an increase in the immune response ($p < 0.001$, $r = 0.633$; Online Resource 2a). To confirm these associations, the levels of immune cytokines were measured by treating HaCaT cells with PM_{2.5} at variable concentrations of 50, 100, and 200 µg/mL for 1, 2, and 4 h, respectively (Online Resource 1b–e). Subsequently, six skin-derived microbes that could significantly reduce the secretion of inflammatory cytokines induced via PM_{2.5} were screened (Online Resource 3). For screening, each concentration was fixed with a 10% concentration of the modified supernatant (Online Resource 1f). IL-1β, IL-6, IL-8, and TNF-α were selected as major screening factors that could contribute to the immune response of keratinocytes. Compared to the levels of four cytokine mRNAs in the untreated HaCaT cells, cytokine secretion was significantly reduced in cells treated with the supernatant derived specifically from the *S. epidermidis* WF2R11 culture medium (Online Resource 4a–d). The mRNA levels of inflammatory cytokines *IL-6*, *IL-8*, *IL-1β*, and *TNF-α*, were significantly reduced in the groups treated with Se solution compared to the respective PM_{2.5} concentrations (50, 100, 200 µg/mL)-treated groups (Fig. 3b–e). Also, upon comparing IL-1β, IL-6, IL-8, and interferon-gamma (IFN-γ) at the protein level, treatment with *S. epidermidis* WF2R11 supernatant significantly reduced protein abundance of all the cytokines mentioned above (Online Resource 4e–h). Taken together, *S. epidermidis* WF2R11 is a skin-bacterium that can significantly reduce the secretion of inflammatory cytokines induced by PM_{2.5}.

Se Solution Suppresses the Accumulation of ROS in HaCaT Cells

To determine whether the Se solution downregulates AhR signaling and reduces ROS production, HaCaT cells were treated with different concentrations of PM_{2.5} (50, 100,

and 200 µg/mL) and inoculated with Se solution. The treatment with Se solution reduced the mRNA level of *AhR* by more than 30% at each PM_{2.5} concentration group (Fig. 4a). Regardless of the concentration of PM_{2.5} treatment, the level of *ARNT* mRNA was similar to that of the control group after treatment with the Se solution (Fig. 4b). As expected, the expression of *CYP1A1* was significantly reduced when inoculated with the Se solution than with only PM_{2.5} (Fig. 4c). In addition, activation of AhR may contribute to the upregulation of Cox-2 expression involved in ROS generation in the cytoplasm [44]. The expression of Cox-2 was significantly increased when PM_{2.5} was treated with 100 µg/ml or more. Moreover, when the Se solution was inoculated to the PM_{2.5}-treated group of the same concentration, the expression level of Cox-2 was significantly reduced (Fig. 4d). Furthermore, JC-1 dye was used to measure the change in mitochondrial membrane potential due to ROS accumulation upon exposure to PM_{2.5}. HaCaT cells stained with JC-1 showed a gradual loss of red J-aggregate fluorescence and cytoplasmic diffusion of green monomeric fluorescence after exposure to accumulated ROS in the cytoplasm. We confirmed that the cytoplasmic diffusion of green monomer fluorescence was significantly reduced when treated with the Se solution of each PM_{2.5} treatment group (Fig. 4e). Based on previous results, we hypothesized that *S. epidermidis* WF2R11 is caused by the inhibition of AhR signaling pathway due to the decrease in intracellular ROS accumulation via PM_{2.5}. Therefore, to investigate the correlation between the *S. epidermidis* WF2R11 and the progression of the AhR signaling pathway, the *AhR* and the *CYP1A1* genes were silenced (ΔAhR and $\Delta CYP1A1$) in HaCaT cells using siRNA.

First, siAhR treatment reduced the mRNA expression levels of *AhR*, *ARNT*, and *CYP1A1* genes to less than half in all other groups compared to the si-control group respectively. However, the *Cox-2* showed a lower mRNA expression level compared to other genes when treated with siAhR. In addition, the expression level of *Cox-2* in the group treated with siAhR and PM_{2.5} was almost similar to that of the si-control group. The mRNA expression was significantly reduced in the Se solution treatment group compared to the PM_{2.5} treatment group (Fig. 4f). Next, we determined whether *S. epidermidis* WF2R11 inhibits AhR alone or regulate sub-mechanisms by silencing the *CYP1A1* gene. When *CYP1A1* was silenced, the mRNA expression levels of *AhR*, *ARNT*, and *Cox-2* showed a similar trend to the previous results (Fig. 4a, b, d). However, the expression of *CYP1A1* gene was significantly lower than that of si-control mRNA in either the PM_{2.5} treatment group or the PM_{2.5} and Se solution treatment group (Fig. 4g). We also observed that the mRNA expression level of *Cox-2* is independent of *CYP1A1* silencing and that the expression of *Cox-2* gene is not directly regulated by *CYP1A1* gene expression. Therefore, the alleviation of PM_{2.5}-derived ROS accumulation



via the AhR signaling pathway of *S. epidermidis* WF2R11 would directly inhibit AhR and down-regulation the sub-gene *CYP1A1*. In addition, we assumed that the regulation of Cox-2

is correlated with other mechanisms according to AhR activity or is affected by the increased intracellular ROS due to increased *CYP1A1* expression.

Fig. 3 *Staphylococcus epidermidis* WF2R11 supernatant (Se solution) reduces the PM_{2.5}-induced immune response. **(a)** Correlation analysis of *AhR* with genes associated with inflammatory responses reveals their positive correlation at the mRNA level. **(b)** Measurement of the mRNA level of *IL-6* cytokine relative to 18S rRNA. **(c)** Measurement of the mRNA level of *IL-8* cytokine relative to 18S rRNA. **(d)** Measurement of the mRNA level of *IL-1β* cytokine relative to 18S rRNA. **(e)** Measurement of the mRNA level of TNF-α cytokine relative to 18S rRNA. The mRNA level of each cytokine relative to 18S rRNA was measured after 12 h of PM_{2.5} treatment or PM_{2.5} and Se solution co-treatment for each concentration. Correlation was determined using Pearson's correlation analysis. Bonferroni test for comparison between pairs was used to calculate statistical significance. #*p* < 0.05, ##*p* < 0.01, ###*p* < 0.001, ns, non-significant; compared to normal HaCaT cells. **p* < 0.05, ***p* < 0.01, ****p* < 0.001, ns, non-significant; compared to each PM_{2.5}-treated group. AhR, aryl hydrocarbon receptor

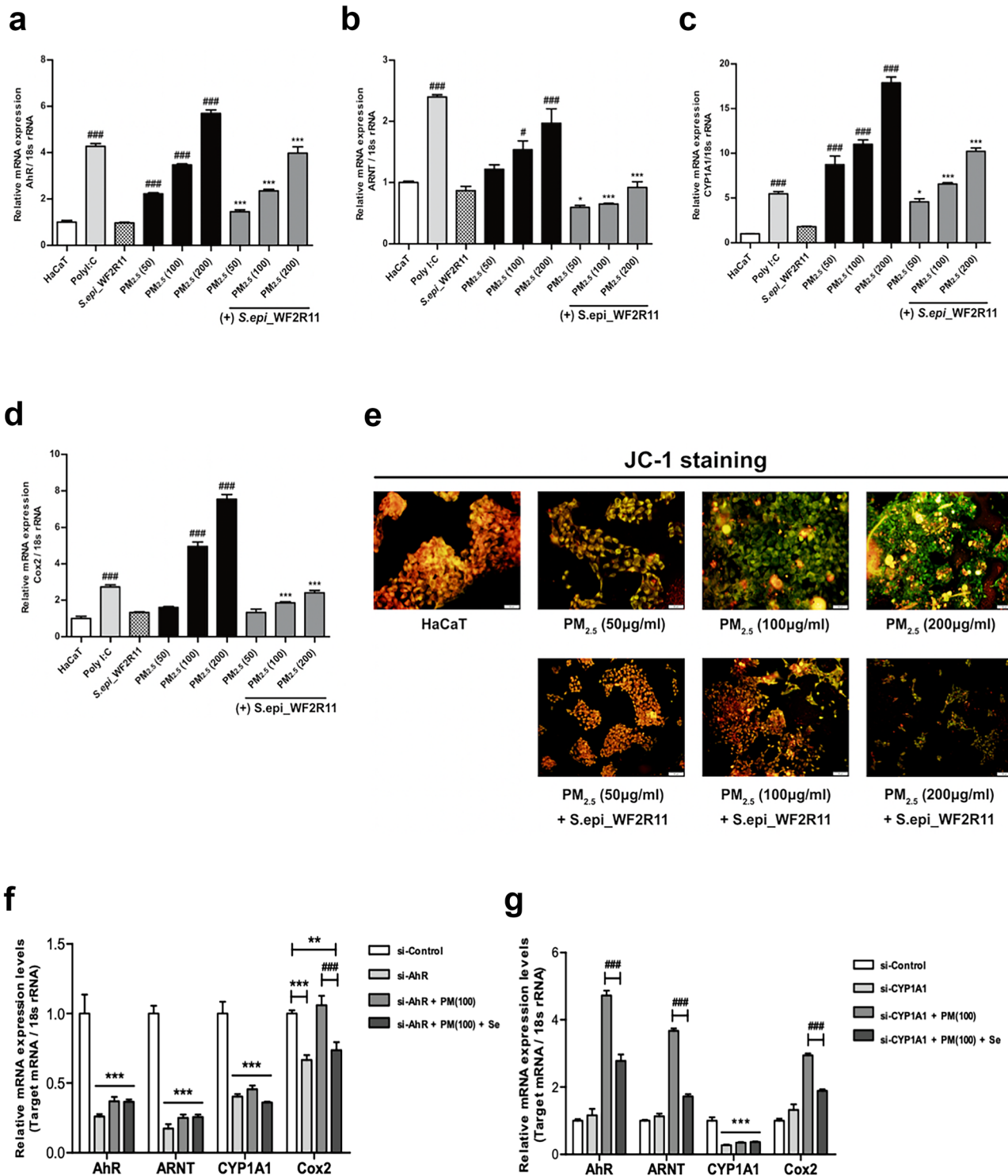
***Staphylococcus epidermidis* WF2R11 Inhibits Mitochondrial Apoptosis Induced by Accumulated Intracellular ROS**

To investigate the mitochondrial apoptosis mechanism of PM_{2.5} mediated by AhR signaling, we assessed the phosphorylation levels of stress-activated protein kinases, such as c-Jun N-terminal kinase (JNK), extracellular signal-regulated kinase 1/2 (ERK), and p38 mitogen-activated protein kinase (p38 kinase). After treatment with either PM_{2.5} (100 μg/ml) or PM_{2.5} (100 μg/ml) and Se solution for 12 h, the phosphorylation level of protein kinase was determined (Fig. 5a). Treatment with PM_{2.5} and Se solution simultaneously decreased both the expression of protein kinases and the degree of phosphorylation compared to PM_{2.5} only treatment. Furthermore, in the same conditions, the Bax protein expression decreased while the Bcl-2 protein expression increased in the group treated with the PM_{2.5} and Se solution compared to that treated with only PM_{2.5}. We quantified the phosphorylation levels of each mitogen-activated protein kinase (MAPK), JNK, ERK, and p38 protein and calculated the Bax/Bcl-2 ratio for correlation with mitochondrial apoptosis mechanisms (Fig. 5b). Although the Bax/Bcl-2 ratio was significantly decreased in normal HaCaT cells compared to the control group (β-actin), the phosphorylation levels of p38 and JNK kinase and the Bax/Bcl-2 ratio were significantly increased following PM_{2.5} treatment.

In addition, Se solution had no effect on MAPKs phosphorylation or Bax/Bcl-2 ratio. Moreover, compared to other skin microbiota, *S. epidermidis* WF2R11 contributed to the observed decrease in mitochondrial Bax expression, which in turn decreased the Bax/Bcl-2 ratio caused by PM_{2.5} treatment (Online Resource 5a–c). However, in the group treated with PM_{2.5} and Se solution simultaneously, the change in the Bax/Bcl-2 ratio and the degree of phosphorylation of MAPKs were not significant compared to the control group. These results suggest that *S. epidermidis* WF2R11 decreased the Bax/Bcl-2 ratio in

PM_{2.5}-treated cells at each concentration, thereby significantly reducing mitochondrial-dependent apoptosis (Fig. 5c). Next, we determined whether PM_{2.5} enables mitochondrial apoptosis via AhR signaling pathway by partially blocking AhR signaling (Fig. 5d). The Bax/Bcl-2 ratio was almost similar in the siAhR-treated group (gray color) regardless of PM_{2.5} or PM_{2.5} and Se solution treatment. However, the siCYP1A1 treatment group (pattern) showed a significant decrease in the Bax/Bcl-2 ratio compared to the si-control group following PM_{2.5} treatment, and a more significant decrease compared to the PM_{2.5} alone treatment group when Se solution was added. Furthermore, when AhR signaling was blocked by treatment with both siAhR and siCYP1A1, the Bax/Bcl-2 ratio was significantly reduced regardless of PM_{2.5} and Se solution treatment. Our results suggest that *CYP1A1* is an important gene that mediates mitochondrial apoptosis signaling induced by PM_{2.5}-induced intracellular ROS accumulation. In addition, *S. epidermidis* WF2R11 directly inhibits AhR to regulate the sub-mechanism of *CYP1A1*-induced sub-mechanisms. To further show that ROS accumulated in HaCaT cells via AhR signaling pathway induced mitochondrial apoptosis, we analyzed apoptosis by treating HaCaT cells with PM_{2.5} and PM_{2.5} and Se solution in siAhR-treated and untreated groups, respectively. We labeled cells with Annexin V-PI and observed the percentage of apoptotic cells using flow cytometry (Fig. 5e) and confirmed that PM_{2.5} alone treatment group significantly increased apoptosis compared to the control group. In addition, PM_{2.5} treatment group to which the Se solution was added showed significant decrease in apoptosis compared to the untreated group. Meanwhile, we treated siAhR-treated cells with PM_{2.5} and analyzed the ratio of apoptosis with and without Se solution. After siAhR treatment, no significant increase in apoptosis was observed in either group treated with PM_{2.5} regardless of Se solution treatment. In the PM_{2.5}-treated group not treated with siAhR, treatment with Se solution shifted the histogram peak from apoptosis state to live state. However, in the PM_{2.5}-treated group with siAhR, the histogram peaks of the two groups overlapped regardless of the Se solution. A significant positive correlation was also observed between the expression of *Cox-2* and the Fas Associated via death domain (*FADD*) gene (*p* < 0.01, *r* = 0.496; Online Resource 5d). In addition to *FADD*, the TNFRSF1A associated via death domain (*TRADD*) gene showed a significant positive correlation with *CYP1A1* (*p* < 0.01, *r* = 0.443; Online Resource 5e).

Ultimately, ROS accumulation via AhR signaling activation could increase *TRADD* gene expression due to mitochondrial-dependent apoptosis through TNF-α signaling (*p* < 0.05, *r* = 0.455; Online Resource 5f).



***Staphylococcus epidermidis* WF2R11 Potentially Affects the Proliferation of HaCaT Cells by Activating Anti-oxidant Activity**

PM_{2.5} is also known to induce DNA damage and apoptosis as well as arrest cell cycle G2/M transition due to

mitochondrial dysfunction [46, 47]. The NF-E2-related factor 2 (Nrf2) and antioxidant response element (ARE) pathway are known to be involved in adaptation to oxidative stress through the upregulation of antioxidant activity and the expression of genes such as NAD(P)H-quinone dehydrogenase 1 (*NQO1*) and heme oxygenase-1 (*HO-1*)

Fig. 4 *Staphylococcus epidermidis* WF2R11 supernatant (Se solution) inhibits apoptosis by inhibiting the AhR signaling pathway and reducing ROS accumulation. Measurement of the mRNA level of (a) *AhR* relative to 18S rRNA, (b) *ARNT* relative to 18S rRNA, (c) *CYP1A1* relative to 18S rRNA, and (d) *Cox-2* relative to 18S rRNA. (e) Measurement of changes in JC-1 fluorescence expression when treated with Se solution compared to either normal HaCaT cells and 50, 100, or 200 µg/mL PM_{2.5} treatment groups. Scale bar, 50 µm. The mRNA level of *AhR*, *ARNT*, *CYP1A1*, and *Cox-2* relative to 18S rRNA was measured after 12 h of PM_{2.5} treatment or PM_{2.5} and Se solution co-treatment for each concentration. #*p* < 0.05, ###*p* < 0.001; compared to normal HaCaT cells. **p* < 0.05, ****p* < 0.001; compared to each PM_{2.5}-treated group. (f) Measurement of the *AhR*, *ARNT*, *CYP1A1*, *Cox-2* relative to 18S rRNA in Δ *AhR* HaCaT cells after 12 h of PM_{2.5} (100 µg/mL) treatment or PM_{2.5} (100 µg/mL) and Se solution co-treatment. (g) Measurement of the *AhR*, *ARNT*, *CYP1A1*, *Cox-2* relative to 18S rRNA in Δ *CYP1A1* HaCaT cells after 12 h of PM_{2.5} (100 µg/mL) treatment or PM_{2.5} (100 µg/mL) and Se solution co-treatment. Bonferroni test for comparison between pairs was used to calculate statistical significance. #*p* < 0.05, ##*p* < 0.01, ###*p* < 0.001, ns, non-significant; comparison between PM_{2.5} treatment and PM_{2.5} and Se solution co-treatment. **p* < 0.05, ***p* < 0.01, ****p* < 0.001; compared to each si-control group

[48–50]. Therefore, transcriptomic analysis was used to investigate the effect of ROS production via AhR signaling activation on the Nrf-2–ARE signaling pathway. Using correlation analysis, the expression of *Nrf-2* was positively correlated with the hallmark genes of the AhR signaling pathway ($p = 0.08$, $r = 0.360$; Online Resource 6a). As a sub-mechanism of Nrf-2–ARE, the expression of *NQO1* ($p = 0.07$, $r = 0.371$; Online Resource 6b) and *HO-1* ($p = 0.01$, $r = 0.485$; Online Resource 6c) genes showed a significant positive correlation with AhR signaling. Consequently, increased expression of *Nrf-2* was ultimately associated with decreased apoptosis ($p < 0.001$, $r = 0.683$; Fig. 5f). The transcriptomic data showed changes in the expression of *Nrf2* and sub-genes (*NQO* and *HO-1*) with or without PM_{2.5} treatment by partially silencing AhR signaling pathway. The expression level of *Nrf2* was correlated with the activation of AhR signaling; meanwhile, when both *AhR* and *CYP1A1* were silenced, the expression level was significantly reduced (Online Resource 6d). Also, when the AhR expression was suppressed in *NQO1* and *HO-1*, the expression level of each gene was reduced to less than half regardless of *CYP1A1* expression (Online Resource 6e, f). Therefore, the direct inhibition of AhR was predicted to be a defense mechanism against ROS, which was promoted through AhR signaling and would eventually prevent apoptosis. As the suppression of apoptosis was expected to affect cell proliferation, Ki-67 immunohistochemistry was performed. The Ki-67 index was more than 70% in the groups inoculated with the five microbial supernatants after PM_{2.5} treatment; whereas, in the PM_{2.5} alone treatment group, the Ki-67 index was approximately 50% (Online Resource 6g). These results showed changes in *Nrf2* expression and confirmed the association of the Nrf-2 signaling pathway by upregulation of AhR

signaling during PM_{2.5} treatment. Moreover, we confirmed the involvement of *S. epidermidis* WF2R11 in HaCaT cell proliferation by participating in AhR-Nrf2 signaling. Thus, we next silenced *AhR* and *CYP1A1* and observed *Nrf2* gene expression following treatment with PM_{2.5} (100 µg/ml), Se solution, and PM_{2.5} (100 µg/ml) and Se solution. The expression of *Nrf2* was significantly decreased in the *AhR* silenced group (gray color) regardless of Se solution treatment with PM_{2.5} compared to the control. However, in the group (pattern) in which *CYP1A1* was silenced, the expression of *Nrf2* was increased more than threefold compared to the control when PM_{2.5} was treated. Meanwhile, when comparing the PM_{2.5}-treated and the Se solution-treated groups, the expression of *Nrf2* was significantly reduced in the Se solution-treated group, although the group in which both *AhR* and *CYP1A1* were silenced (black color) showed almost no expression of *Nrf2* regardless of PM_{2.5} and Se solution treatment (Fig. 5g). Taken together, these results suggest that *S. epidermidis* WF2R11 effectively inhibited ROS production through AhR signaling and caused a decrease in apoptosis. In this process, the Nrf-2 signaling pathway, a part of AhR signaling, was directly/indirectly upregulated based on AhR signaling and ROS generation, affecting the regulation of cell proliferation as well as mitochondrial-dependent cell death (Fig. 6).

Discussion

This study demonstrated the effect of PM_{2.5} exposure on the AhR pathway and mitochondrial dysfunction-dependent apoptosis. To the best of our knowledge, this is the first study to analyze how a member of skin microbiota can downregulate the AhR pathway, which leads to the inhibition of skin inflammation and ROS production. We specifically investigated the effect of *S. epidermidis* WF2R11 on the progression of the AhR pathway. The main mechanism by which PM_{2.5} induces cellular oxidative stress is through the generation of ROS in skin keratinocytes [51]. PM_{2.5} directly increases the level of ROS production and free radicals on the surface of skin keratinocytes, indicating potent redox activity in PAHs [52, 53]. In addition, oxy-PAH reportedly promotes the oxidation of nucleic acids, proteins, and lipids more than PAH, which can cause severe redox stress in cells and tissues [54, 55]. Water-soluble PAHs such as BaP, unlike other organic compounds, tend to oxidize rapidly [56], and oxy-PAHs show increased cell permeability and AhR reactivity [26]. Initiation of AhR-mediated signaling by PAHs or oxy-PAHs is first transferred to the nucleus upon binding of the PM_{2.5}-binding AhR complexes to ARNT [26, 57]. It was evident that, when PM_{2.5} acted as a ligand for AhR, both the AhR and ARNT mRNA levels increased. Our results demonstrated that although *S. epidermidis* WF2R11 did not

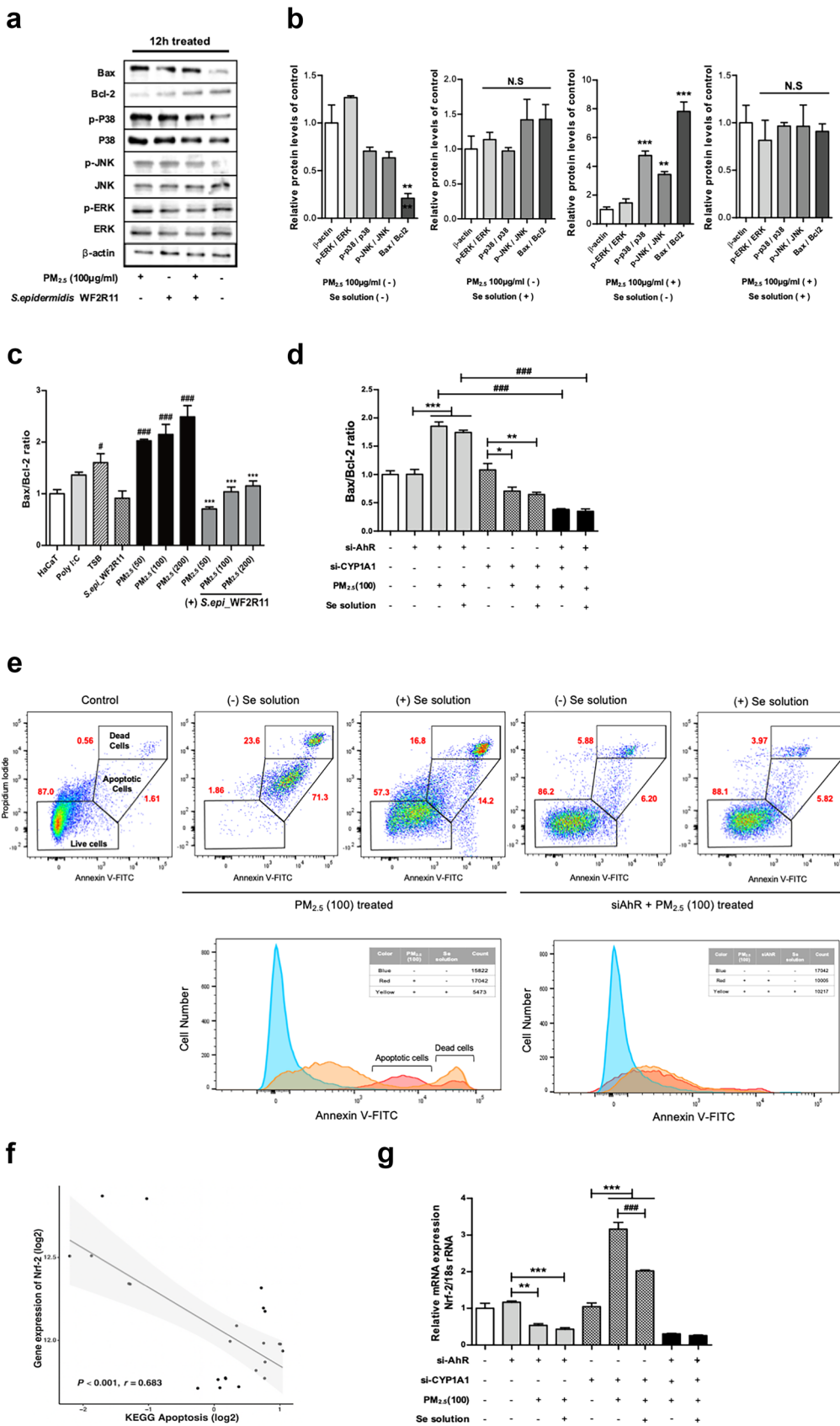


Fig. 5 *Staphylococcus epidermidis* WF2R11 supernatant (Se solution) directly downregulates AhR and affects cell proliferation. **(a)** The protein expression of MAPK pathway-related proteins including p-p38, p38, p-JNK, JNK, p-ERK, ERK was detected via Western blot. **(b)** Quantitative analysis of p-ERK/ERK, p-p38/p38, and p-JNK/JNK based on Western blot results. ** $p < 0.01$, *** $p < 0.001$, ns, non-significant; compared to internal control; β -actin. **(c)** Measurement of the relative *Bax/Bcl-2* ratio level in response to mitochondrial-dependent cell death in the PM_{2.5} treatment group and Se solution treatment group. # $p < 0.05$, ### $p < 0.001$; compared to normal HaCaT cells. *** $p < 0.001$; compared to each PM_{2.5}-treated group. **(d)** Measurement of the relative *Bax/Bcl-2* ratio in Δ AhR, Δ CYP1A1, and when both genes are silenced in HaCaT cells after 12 h of PM_{2.5} (100 μ g/mL) treatment or PM_{2.5} (100 μ g/mL) and Se solution co-treatment. * $p < 0.05$, ** $p < 0.01$, *** $p < 0.001$; compared to each si-control group. ### $p < 0.001$; comparison between PM_{2.5} treatment and PM_{2.5} and Se solution co-treatment. **(e)** Visualization of the effect of Se solution treatment on apoptosis of siAhR-treated or untreated HaCaT cells during PM_{2.5} treatment using Annexin V-Pi staining. Representative scatterplot and histogram analysis data are shown. **(f)** Correlation analysis of Nrf-2 with KEGG-apoptosis reveals its negative correlation at the mRNA level. **(g)** Measurement of the mRNA level of *Nrf-2* relative to 18S rRNA in Δ AhR, Δ CYP1A1, and both genes are silenced in HaCaT cells. ** $p < 0.01$, *** $p < 0.001$; compared to each si-control group. ### $p < 0.001$; comparison between PM_{2.5} treatment and PM_{2.5} and Se solution co-treatment. Bonferroni test for comparison between pairs was used to calculate statistical significance. Correlation was determined using Pearson's correlation analysis

directly affect AhR, it reduced *AhR* and *ARNT* mRNA levels. It was initially speculated that the reduced expression of *AhR* and *ARNT* is caused by the metabolites secreted by *S. epidermidis* WF2R11, thereby affecting the formation of AhR/ARNT complexes. However, when *AhR* was knocked down in HaCaT cells, *ARNT* and *CYP1A1* expression was inhibited regardless of treatment with PM_{2.5} or the *S. epidermidis* WF2R11 supernatant. Although previous hypotheses have speculated that the *S. epidermidis* WF2R11 metabolites inhibit the formation of the AhR/ARNT complex, this finding demonstrated that AhR activation to PAH is a prerequisite for *ARNT* and *CYP1A1* expression. We therefore suggest that the *S. epidermidis* WF2R11 metabolites may operate by suppressing AhR activity on PAHs or act as a competitive ligand inhibitor, rather than directly inhibiting the formation of the AhR/ARNT complexes. AhR/ARNT heterodimers bind to xenobiotic responsive elements and activate the transcription of sub-target genes such as *CYP1* [58]. CYP1 is a key factor capable of promoting ROS accumulation in the cytoplasm, concomitantly causing oxidative stress [59, 60]. In addition, CYP enzymes induce ROS accumulation in the cytoplasm by damaging keratinocytes and altering DNA formation [25, 37, 61]. The mRNA level of *CYP1A1* was significantly increased after PM_{2.5} treatment, while *S. epidermidis* WF2R11 was involved in the inhibition of AhR activity, thereby reducing the expression of *CYP1A1*. Thus, the AhR/ARNT complex affects the activity of the CYP1 enzyme, thereby increasing the expression of *CYP1A1* [39, 62]. In addition, cytoplasmic ROS production by *Cox-2*

overexpression in HaCaT cells critically exerts oxidative stress on various organelles, including mitochondria [59, 63]. Signaling due to AhR activity was associated with an increase in *CYP1A1* and in *Cox-2* expression [64]. In particular, when AhR was silenced, the expression of *Cox-2* was significantly reduced, which was restored following PM_{2.5} treatment to the same level as that of si-control. However, despite silencing *CYP1A1*, signal transduction of AhR caused an increase in the expression of *Cox-2*, which suggests that the expression of *Cox-2* is determined somewhat independently of the sub-mechanism of *CYP1A1*, and its expression may be regulated by AhR activity. Moreover, PAH and oxy-PAH result in differential ROS generation and Ca²⁺ perturbation and promote electrophysiological instability, which increases mitochondrial inner membrane permeability. Furthermore, an increase in ROS not only produce a cytotoxic effect, but also activate MAPK pathways, including JNK, ERK, and p38 MAPK, which ultimately lead to mitochondrial stress and excessive free radical accumulation, resulting in mitochondrial dysfunction and apoptosis (i.e., the intrinsic pathway of apoptosis) [65–69]. We visualized mitochondrial superoxide and membrane potential after PM_{2.5} and Se solution treatment via fluorescent staining (Mito-Sox, JC-1), suggesting that the metabolite of *S. epidermidis* WF2R11 is effective in suppressing PM_{2.5}-induced oxidative stress. Furthermore, we demonstrated that the metabolites of *S. epidermidis* WF2R11 can significantly reduce phosphorylation of p38 kinase and JNK among ROS-activated MAPK subgroups. Bax is phosphorylated by stress-activated p38 kinase and/or JNK and phosphorylation of Bax leads to mitochondrial translocation prior to apoptosis. The mitochondrial translocation of pro-apoptotic Bax can act as apoptosis stimulators or conditions that induce mitochondrial apoptosis [70, 71]. PM_{2.5}-induced apoptosis upregulates *Bax* and downregulates *Bcl-2* [68, 72–74]; therefore, a decrease in the *Bax/Bcl-2* ratio suggests a decrease in mitochondrial dysfunction-dependent apoptosis in the *S. epidermidis* WF2R11-treated group. Although the mechanism by which increased ROS can activate ERK, JNK and p38 MAPK remain unclear [75], we found that groups treated with *S. epidermidis* WF2R11 did not show any significant difference in the regulation of *Bcl-2* but exhibited downregulated *Bax* expression. In addition, since the PM_{2.5}-derived ROS-induced mitochondrial apoptosis mechanism is increased through the AhR signaling pathway, the change in the *Bax/Bcl-2* ratio was confirmed after suppressing the *AhR* or *CYP1A1* gene, or both. We confirmed that the key gene for PM_{2.5}-derived ROS increase was the expression of *CYP1A1*, while *S. epidermidis* WF2R11 suppressed AhR, the upper gene of *CYP1A1*, to reduce PM_{2.5}-derived ROS. Transcriptome analysis showed that the AhR signaling pathway not only increased the expression of *CYP1A1* but

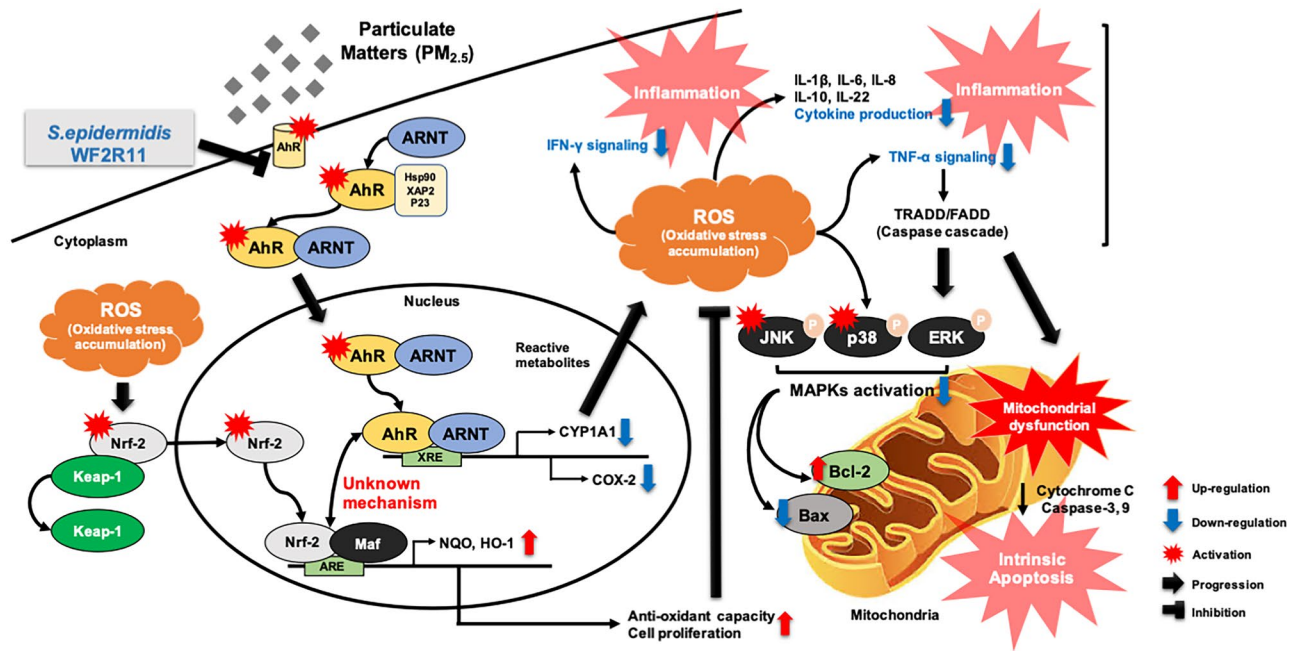


Fig. 6 Schematic illustration showing the effect of *Staphylococcus epidermidis* WF2R11 on the intracellular changes induced by PM_{2.5}. XRE, xenobiotic-binding factor; AhR, aryl hydrocarbon receptor; ARNT, AhR nuclear translocator; CYP1A1, cytochrome P450 family

1 subfamily A member 1; Cox-2, cyclooxygenase-2; Nrf-2, nuclear factor erythroid 2-related factor 2; ROS, reactive oxygen species; JNK, c-Jun N-terminal kinase; p38, p38 mitogen-activated protein kinase; ERK, extracellular signal-regulated kinase

also contributed to the activation of TNF- α signaling to induce mitochondrial apoptosis, or upregulate *Cox-2*, thereby contributing to the activity of p38 and JNK MAPKs to enable translocation of mitochondrial *Bax*. Taken together, excessive oxidative stress due to the AhR pathway specifically affects the expression level of *Bax* via phosphorylation of MAPKs and may be a major contributor to mitochondrial dysfunction [76–78]. The reduction of oxidative stress, resulting from inhibition of AhR pathway progression, may have an inhibitory effect on the upregulation of *Bax*, which suggests AhR as an important receptor that leads to apoptosis by causing mitochondrial dysfunction. Furthermore, the metabolites of *S. epidermidis* WF2R11 can inhibit the progression of ROS-mediated damage by reducing AhR activity. Endogenous ROS can also cause structural damage and cell degradation, leading to apoptosis in HaCaT cells [33]. Previous studies showed that mitochondrial dysfunction caused by PM_{2.5} triggers an inflammatory cascade [34]. Activated Toll-like receptors initiate the NF- κ B pathway and secrete inflammatory cytokines such as IL-1 α , IL-1 β , IL-6, IL-8, and TNF- α [79]. The secretion of these cytokines promotes the rapid activity of inflammatory reactions. Activated NF- κ B initiates an inflammatory cascade, which causes the skin barrier to collapse, aggravating skin inflammation and leading to apoptosis [17, 80, 81]. The finding of this study suggests that AhR regulation of microbial metabolites is expected to help alleviate these inflammatory responses.

Finally, we confirmed whether *S. epidermidis* WF2R11 effectively reduced apoptosis and inflammatory responses from PM_{2.5}-induced oxidative stress via AhR-mediated Nrf2 signaling. Previous studies have suggested two different mechanisms for the activation of Nrf2 by AhR: direct transcriptional activation of Nrf2 following AhR signaling activation or ROS generation by *CYP1A1* induction [82, 83]. Among these two hypotheses, we investigated the pathway by which metabolites of *S. epidermidis* WF2R11 influence initiation of Nrf2 signaling. AhR silencing significantly reduced the expression level of Nrf2 and sub-genes such as *NQO1* and *HO-1* regardless of PM_{2.5} or *S. epidermidis* WF2R11 treatment. However, when *CYP1A1* was silenced, while treating with PM_{2.5}, the expression of Nrf2 gene was significantly increased, whereas when PM_{2.5} and *S. epidermidis* WF2R11 were co-treated, the expression of Nrf2 was significantly decreased.

These results indicate that AhR, not *CYP1A1*, has direct transcriptional activation function for Nrf2 signal and that two other pathways of AhR may be activated simultaneously, one to increase cellular ROS and the other to trigger an antioxidant response. Furthermore, the decrease in expression Nrf2 following inhibition of AhR may possibly reduce the activation signal for other ROS generation mechanisms involved in the AhR signaling pathway. Conversely, we consider that the reason for the increase in Nrf2 during PM_{2.5} treatment despite the silencing of

CYP1A1 is probably attributed to ROS generation associated with the increased expression of *Cox-2* based on the activity of AhR. Thus, the direction of pathway progression of AhR will depend on either the ligand, intracellular ROS accumulation, or additional factors, which will determine the agonist or compensatory antioxidant AhR pathway.

Taken together, these findings provide new insights into the potential application of skin microbiome interventions in clinical practice. However, this study could not comprehensively explore the mechanism by which the metabolites of *S. epidermidis* WF2R11 can inhibit the activation of AhR. Therefore, further research is required to study the effects of metabolites secreted by the skin microbiome on the AhR signaling pathway. We will also investigate the association of AhR-Trp metabolism and explore the functional significance of microbial Trp metabolites in skin inflammation. Future studies should harbor the prospect of overcoming these limitations and treating skin diseases caused by PM_{2.5} exposure.

Supplementary Information The online version contains supplementary material available at <https://doi.org/10.1007/s12602-022-09922-8>.

Acknowledgements The authors thank the Labcore Company (Seoul, Korea) for their expertise in immunohistochemical staining.

Author Contribution Eulgi Lee performed qPCR and in vitro cell assays, analyzed the RNA sequences, prepared the figures, and wrote the manuscript. Shinyoung Park isolated whole skin microbiomes and the product of the supernatants. Myung-Giun Noh analyzed the immunohistochemistry results. Hyeok Ahn, Yunjae Kim, Hyun Kim, Gihyeon Kim, and Jae-sung Yeon performed in vitro cell assays and qPCR. Hansoo Park designed and supervised all experiments and analyses.

Funding This research was supported by the research collaboration between Gwangju Institute of Science and Technology (GIST) Research Institute (GRI) and Chonnam National University Hospital (CNUH) (grant number GK12640).

Availability of Data and Material All processed gene expression data used in this study were procured from the Gene Expression Omnibus under accession number GSE107871.

Declarations

Ethics Approval This study was approved by the Institutional Review Board (IRB: P01-201605–31-003) of Korea National Institute for Bioethics Policy (KONIBP). The study was performed in accordance with the ethical standards as laid down in the declaration of Helsinki and also all study protocols adhered to relevant ethical guidelines.

Consent to Participate All participants provided written informed consent before enrolment.

Conflict of Interest The authors declare no competing interests.

Open Access This article is licensed under a Creative Commons Attribution 4.0 International License, which permits use, sharing, adaptation, distribution and reproduction in any medium or format, as long as you give appropriate credit to the original author(s) and the source, provide a link to the Creative Commons licence, and indicate if changes were made. The images or other third party material in this article are included in the article's Creative Commons licence, unless indicated otherwise in a credit line to the material. If material is not included in the article's Creative Commons licence and your intended use is not permitted by statutory regulation or exceeds the permitted use, you will need to obtain permission directly from the copyright holder. To view a copy of this licence, visit <http://creativecommons.org/licenses/by/4.0/>.

References

- Hoffmann B et al (2009) Chronic residential exposure to particulate matter air pollution and systemic inflammatory markers. *Environ Health Perspect* 117(8):1302–1308. <https://doi.org/10.1289/ehp.0800362>
- Davidson CI, Phalen RF, Solomon PA (2005) Airborne particulate matter and human health: a review. *Aerosol Sci Technol* 39(8):737–749. <https://doi.org/10.1080/02786820500191348>
- Adams K et al (2015) Particulate matter components, sources, and health: systematic approaches to testing effects. *J Air Waste Manag Assoc* 65(5):544–558. <https://doi.org/10.1080/10962247.2014.1001884>
- De Kok TM et al (2006) Toxicological assessment of ambient and traffic-related particulate matter: a review of recent studies. *Mutat Res* 613(2–3):103–122. <https://doi.org/10.1016/j.mrrev.2006.07.001>
- Oberdörster G (2001) Pulmonary effects of inhaled ultrafine particles. *Int Arch Occup Environ Health* 74(1):1–8. <https://doi.org/10.1007/s004200000185>
- Barnard E, Li H (2017) Shaping of cutaneous function by encounters with commensals. *J Physiol* 595(2):437–450. <https://doi.org/10.1113/JP271638>
- Sanford JA, Gallo RL (2013) Functions of the skin microbiota in health and disease. In: *Semin Immunol*. Elsevier 25(5):370–377. <https://doi.org/10.1016/j.smim.2013.09.005>
- Kong HH (2011) Skin microbiome: genomics-based insights into the diversity and role of skin microbes. *Trends Mol Med* 17(6):320–328. <https://doi.org/10.1016/j.molmed.2011.01.013>
- Paulino LC et al (2006) Molecular analysis of fungal microbiota in samples from healthy human skin and psoriatic lesions. *J Clin Microbiol* 44(8):2933–2941. <https://doi.org/10.1128/JCM.00785-06>
- Brüggemann H et al (2004) The complete genome sequence of *Propionibacterium acnes*, a commensal of human skin. *Science* 305(5684):671–673. <https://doi.org/10.1126/science.1100330>
- Holland KT, Greenman J, Cunliffe WJ (1979) Growth of cutaneous propionibacteria on synthetic medium; growth yields and exoenzyme production. *J Appl Bacteriol* 47(3):383–394. <https://doi.org/10.1111/j.1365-2672.1979.tb01198.x>
- Ingham E et al (1981) Partial purification and characterization of lipase (EC 3.1. 1.3) from *Propionibacterium acnes*. *J Gen Microbiol* 124(2):393–401. <https://doi.org/10.1099/00221287-124-2-393>
- Marples RR, Downing DT, Kligman AM (1971) Control of free fatty acids in human surface lipids by *Corynebacterium acnes*. *J Invest Dermatol* 56(2):127–131. <https://doi.org/10.1111/1523-1747.ep12260695>
- Gibbon EM, Cunliffe WJ, Holland KT (1993) Interaction of *Propionibacterium acnes* with skin lipids *in vitro*. *J Gen Microbiol* 139(8):1745–1751. <https://doi.org/10.1099/00221287-139-8-1745>

15. Iebba V et al (2016) Eubiosis and dysbiosis: the two sides of the microbiota. *New Microbiol* 39(1):1–12
16. Mukherjee S et al (2016) Sebum and hydration levels in specific regions of human face significantly predict the nature and diversity of facial skin microbiome. *Sci Rep* 6:36062. <https://doi.org/10.1038/srep36062>
17. Jin SP et al (2018) Urban particulate matter in air pollution penetrates into the barrier-disrupted skin and produces ROS-dependent cutaneous inflammatory response *in vivo*. *J Dermatol Sci* 91(2):175–183. <https://doi.org/10.1016/j.jdermsci.2018.04.015>
18. Lundstedt S et al (2007) Sources, fate, and toxic hazards of oxygenated polycyclic aromatic hydrocarbons (PAHs) at PAH-contaminated sites. *AMBIO J Hum Environ* 36(6):475–485. [https://doi.org/10.1579/0044-7447\(2007\)36\[475:sfatho\]2.0.co;2](https://doi.org/10.1579/0044-7447(2007)36[475:sfatho]2.0.co;2)
19. Nebert DW et al (2000) Role of the aromatic hydrocarbon receptor and [Ah] gene battery in the oxidative stress response, cell cycle control, and apoptosis. *Biochem Pharmacol* 59(1):65–85. [https://doi.org/10.1016/s0006-2952\(99\)00310-x](https://doi.org/10.1016/s0006-2952(99)00310-x)
20. Marlowe JL, Puga A (2005) Aryl hydrocarbon receptor, cell cycle regulation, toxicity, and tumorigenesis. *J Cell Biochem* 96(6):1174–1184. <https://doi.org/10.1002/jcb.20656>
21. Bosetti C, Boffetta P, La Vecchia C (2007) Occupational exposures to polycyclic aromatic hydrocarbons, and respiratory and urinary tract cancers: a quantitative review to 2005. *Ann Oncol* 18(3):431–446. <https://doi.org/10.1093/annonc/mdl172>
22. Poursafa P et al (2017) A systematic review on the effects of polycyclic aromatic hydrocarbons on cardiometabolic impairment. *Int J Prev Med* 8:19. https://doi.org/10.4103/ijpvm.IJPVM_144_17
23. Brucker N et al (2014) Atherosclerotic process in taxi drivers occupationally exposed to air pollution and co-morbidities. *Environ Res* 131:31–38. <https://doi.org/10.1016/j.envres.2014.02.012>
24. Wincent E, Le Bihanic F, Dreij K (2016) Induction and inhibition of human cytochrome P4501 by oxygenated polycyclic aromatic hydrocarbons. *Toxicol Res (Camb)* 5(3):788–799. <https://doi.org/10.1039/c6tx00004e>
25. Shimada T, Fujii-Kuriyama Y (2004) Metabolic activation of polycyclic aromatic hydrocarbons to carcinogens by cytochromes P450 1A1 and 1B1. *Cancer Sci* 95(1):1–6. <https://doi.org/10.1111/j.1349-7006.2004.tb03162.x>
26. Ju S et al (2020) Oxygenated polycyclic aromatic hydrocarbons from ambient particulate matter induce electrophysiological instability in cardiomyocytes. *Part Fibre Toxicol* 17(1):25. <https://doi.org/10.1186/s12989-020-00351-5>
27. Piao MJ et al (2018) Particulate matter 2.5 damages skin cells by inducing oxidative stress, subcellular organelle dysfunction, and apoptosis. *Arch Toxicol* 92(6):2077–2091. <https://doi.org/10.1007/s00204-018-2197-9>
28. Chin BY et al (1998) Induction of apoptosis by particulate matter: role of TNF- α and MAPK. *Am J Physiol* 275(5):L942–L949. <https://doi.org/10.1152/ajplung.1998.275.5.L942>
29. Mastrofrancesco A et al (2014) Proinflammatory effects of diesel exhaust nanoparticles on scleroderma skin cells. *J Immunol Res* 2014:138751. <https://doi.org/10.1155/2014/138751>
30. Mohan S et al (2010) *Typhonium flagelliforme* induces apoptosis in CEMss cells via activation of caspase-9, PARP cleavage and cytochrome c release: its activation coupled with G0/G1 phase cell cycle arrest. *J Ethnopharmacol* 131(3):592–600. <https://doi.org/10.1016/j.jep.2010.07.043>
31. Simon HU, Haj-Yehia A, Levi-Schaffer F (2000) Role of reactive oxygen species (ROS) in apoptosis induction. *Apoptosis* 5(5):415–418. <https://doi.org/10.1023/a:1009616228304>
32. Su CG et al (1999) A novel therapy for colitis utilizing PPAR- γ ligands to inhibit the epithelial inflammatory response. *J Clin Invest* 104(4):383–389. <https://doi.org/10.1172/JCI7145>
33. Redza-Dutordoir M, Averill-Bates DA (2016) Activation of apoptosis signalling pathways by reactive oxygen species. *Biochim Biophys Acta Mol Cell Res* 1863(12):2977–2992. <https://doi.org/10.1016/j.bbamcr.2016.09.012>
34. Xia T, Kovoichich M, Nel AE (2007) Impairment of mitochondrial function by particulate matter (PM) and their toxic components: implications for PM-induced cardiovascular and lung disease. *Front Biosci* 12(1):1238–1246. <https://doi.org/10.2741/2142>
35. Larigot L et al (2018) AhR signaling pathways and regulatory functions. *Biochim Open* 7:1–9. <https://doi.org/10.1016/j.biopen.2018.05.001>
36. Swindell W (2017) RNA-seq identifies a diminished differentiation gene signature in 1092 primary monolayer keratinocytes grown from lesional and uninvolved psoriatic skin. *Sci* 1093(7):18045
37. Costa C et al (2010) Exposure of human skin to benzo [a] pyrene: role of CYP1A1 and aryl hydrocarbon receptor in oxidative stress generation. *Toxicology* 271(3):83–86. <https://doi.org/10.1016/j.tox.2010.02.014>
38. Ranjit S et al (2018) Benzo (a) pyrene in cigarette smoke enhances HIV-1 replication through NF- κ B activation via CYP-mediated oxidative stress pathway. *Sci Rep* 8(1):10394. <https://doi.org/10.1038/s41598-018-28500-z>
39. Huang P, Ceccatelli S, Rannug A (2002) A study on diurnal mRNA expression of CYP1A1, AHR, ARNT, and PER2 in rat pituitary and liver. *Environ Toxicol Pharmacol* 11(2):119–126. [https://doi.org/10.1016/s1382-6689\(01\)00111-9](https://doi.org/10.1016/s1382-6689(01)00111-9)
40. Magnani ND et al (2013) Reactive oxygen species produced by NADPH oxidase and mitochondrial dysfunction in lung after an acute exposure to residual oil fly ashes. *Toxicol Appl Pharmacol* 270(1):31–38. <https://doi.org/10.1016/j.taap.2013.04.002>
41. Ali D et al (2018) ROS-dependent Bax/Bcl2 and caspase 3 pathway-mediated apoptosis induced by zineb in human keratinocyte cells. *Onco Targets Ther* 11:489–497. <https://doi.org/10.2147/OTT.S140358>
42. Han LL et al (2009) Reactive oxygen species production and Bax/Bcl-2 regulation in honokiol-induced apoptosis in human hepatocellular carcinoma SMMC-7721 cells. *Environ Toxicol Pharmacol* 28(1):97–103. <https://doi.org/10.1016/j.etap.2009.03.005>
43. Perlman H et al (1999) An elevated Bax/bcl-2 ratio corresponds with the onset of prostate epithelial cell apoptosis. *Cell Death Differ* 6(1):48–54. <https://doi.org/10.1038/sj.cdd.4400453>
44. Hanieh H (2014) Toward understanding the role of aryl hydrocarbon receptor in the immune system: current progress and future trends. *BioMed Res Int* 2014:520763. <https://doi.org/10.1155/2014/520763>
45. Quintana FJ, Sherr DH (2013) Aryl hydrocarbon receptor control of adaptive immunity. *Pharmacol Rev* 65(4):1148–1161. <https://doi.org/10.1124/pr.113.007823>
46. Familiari M et al (2019) Exposure of trophoblast cells to fine particulate matter air pollution leads to growth inhibition, inflammation and ER stress. *PLoS One* 14(7):e0218799. <https://doi.org/10.1371/journal.pone.0218799>
47. Qin Z et al (2017) Fine particulate matter exposure induces cell cycle arrest and inhibits migration and invasion of human extravillous trophoblast, as determined by an iTRAQ-based quantitative proteomics strategy. *Reprod Toxicol* 74:10–22. <https://doi.org/10.1016/j.reprotox.2017.08.014>
48. Bajpai VK et al (2017) Antioxidant efficacy and the upregulation of Nrf2-mediated HO-1 expression by (+)-lariciresinol, a lignan isolated from *Rubia philippinensis*, through the activation of p38. *Sci Rep* 7(1):46035. <https://doi.org/10.1038/srep46035>
49. Li L et al (2014) Nrf2/ARE pathway activation, HO-1 and NQO1 induction by polychlorinated biphenyl quinone is associated with reactive oxygen species and PI3K/AKT signaling. *Chem Biol Interact* 209:56–67. <https://doi.org/10.1016/j.cbi.2013.12.005>
50. Loboda A et al (2016) Role of Nrf2/HO-1 system in development, oxidative stress response and diseases: an evolutionarily

- conserved mechanism. *Cell Mol Life Sci* 73(17):3221–3247. <https://doi.org/10.1007/s00018-016-2223-0>
51. Schieber M, Chandel NS (2014) ROS function in redox signaling and oxidative stress. *Curr Biol* 24(10):R453–R462. <https://doi.org/10.1016/j.cub.2014.03.034>
 52. Fang T et al (2019) Oxidative potential of particulate matter and generation of reactive oxygen species in epithelial lining fluid. *Environ Sci Technol* 53(21):12784–12792. <https://doi.org/10.1021/acs.est.9b03823>
 53. Øvrevik J et al (2015) Activation of proinflammatory responses in cells of the airway mucosa by particulate matter: oxidant- and non-oxidant-mediated triggering mechanisms. *Biomolecules* 5(3):1399–1440. <https://doi.org/10.3390/biom5031399>
 54. Stockfelt L et al (2017) Long-term effects of total and source-specific particulate air pollution on incident cardiovascular disease in Gothenburg, Sweden. *Environ Res* 158:61–71. <https://doi.org/10.1016/j.envres.2017.05.036>
 55. Du Y et al (2016) Air particulate matter and cardiovascular disease: the epidemiological, biomedical and clinical evidence. *J Thorac Dis* 8(1):E8–E19. <https://doi.org/10.3978/j.issn.2072-1439.2015.11.37>
 56. Wang L, Atkinson R, Arey J (2007) Formation of 9, 10-phenanthrenequinone by atmospheric gas-phase reactions of phenanthrene. *Atmos Environ* 41(10):2025–2035. <https://doi.org/10.1016/j.atmosenv.2006.11.008>
 57. Redaelli C et al (2015) Toxicity of terflunomide in aryl hydrocarbon receptor deficient mice. *Biochem Pharmacol* 98(3):484–492. <https://doi.org/10.1016/j.bcp.2015.08.111>
 58. Schulte KW et al (2017) Structural basis for aryl hydrocarbon receptor-mediated gene activation. *Structure* 25(7):1025–1033.e3. <https://doi.org/10.1016/j.str.2017.05.008>
 59. Cillero-Pastor B et al (2008) Mitochondrial dysfunction activates cyclooxygenase 2 expression in cultured normal human chondrocytes. *Arthritis Rheum* 58(8):2409–2419. <https://doi.org/10.1002/art.23644>
 60. Totlandsdal AI et al (2010) Diesel exhaust particles induce CYP1A1 and pro-inflammatory responses via differential pathways in human bronchial epithelial cells. *Part Fibre Toxicol* 7(1):41. <https://doi.org/10.1186/1743-8977-7-41>
 61. Ranjit S et al (2016) Effect of polyaryl hydrocarbons on cytotoxicity in monocytic cells: potential role of cytochromes P450 and oxidative stress pathways. *PLoS One* 11(9):e0163827. <https://doi.org/10.1371/journal.pone.0163827>
 62. Manzella C et al (2018) Serotonin is an endogenous regulator of intestinal CYP1A1 via AhR. *Sci Rep* 8(1):6103. <https://doi.org/10.1038/s41598-018-24213-5>
 63. Kiritoshi S et al (2003) Reactive oxygen species from mitochondria induce cyclooxygenase-2 gene expression in human mesangial cells: potential role in diabetic nephropathy. *Diabetes* 52(10):2570–2577. <https://doi.org/10.2337/diabetes.52.10.2570>
 64. Degner SC et al (2007) Cyclooxygenase-2 promoter activation by the aromatic hydrocarbon receptor in breast cancer mcf-7 cells: repressive effects of conjugated linoleic acid. *Nutr Cancer* 59(2):248–257. <https://doi.org/10.1080/01635580701485585>
 65. Karakoçak BB et al (2019) Investigating the effects of stove emissions on ocular and cancer cells. *Sci Rep* 9(1):1870. <https://doi.org/10.1038/s41598-019-38803-4>
 66. Nishitoh H (2012) CHOP is a multifunctional transcription factor in the ER stress response. *J Biochem* 151(3):217–219. <https://doi.org/10.1093/jb/mvr143>
 67. Pfaffenbach KT, Lee AS (2011) The critical role of GRP78 in physiologic and pathologic stress. *Curr Opin Cell Biol* 23(2):150–156. <https://doi.org/10.1016/j.cob.2010.09.007>
 68. Piao MJ et al (2019) Particulate matter 2.5 mediates cutaneous cellular injury by inducing mitochondria-associated endoplasmic reticulum stress: protective effects of ginsenoside Rb1. *Antioxidants (Basel)* 8(9):383. <https://doi.org/10.3390/antiox8090383>
 69. Seok JK et al (2018) Punicalagin and (–)-epigallocatechin-3-gallate rescue cell viability and attenuate inflammatory responses of human epidermal keratinocytes exposed to airborne particulate matter PM10. *Skin Pharmacol Physiol* 31(3):134–143. <https://doi.org/10.1159/000487400>
 70. Kim BJ, Ryu SW, Song BJ (2006) JNK-and p38 kinase-mediated phosphorylation of Bax leads to its activation and mitochondrial translocation and to apoptosis of human hepatoma HepG2 cells. *J Biol Chem* 281(30):21256–21265. <https://doi.org/10.1074/jbc.M510644200>
 71. Van Laethem A et al (2004) Activation of p38 MAPK is required for Bax translocation to mitochondria, cytochrome c release and apoptosis induced by UVB irradiation in human keratinocytes. *FASEB J* 18(15):1946–1948. <https://doi.org/10.1096/fj.04-2285fje>
 72. Ryu YS et al (2019) Particulate matter-induced senescence of skin keratinocytes involves oxidative stress-dependent epigenetic modifications. *Exp Mol Med* 51(9):1–14. <https://doi.org/10.1038/s12276-019-0305-4>
 73. Zhen AX et al (2019) Eckol inhibits particulate matter 2.5-induced skin keratinocyte damage via MAPK signaling pathway. *Mar Drugs* 17(8):444. <https://doi.org/10.3390/md17080444>
 74. Zhen AX et al (2019) Diphlorethohydroxycarmalol attenuates fine particulate matter-induced subcellular skin dysfunction. *Mar Drugs* 17(2):95. <https://doi.org/10.3390/md17020095>
 75. Son Y et al (2013) Reactive oxygen species in the activation of MAP kinases. *Methods Enzymol* 528:27–48. <https://doi.org/10.1016/B978-0-12-405881-1.00002-1>
 76. Cui H, Kong Y, Zhang H (2012) Oxidative stress, mitochondrial dysfunction, and aging. *J Signal Transduct* 2012:646354. <https://doi.org/10.1155/2012/646354>
 77. Guo C et al (2013) Oxidative stress, mitochondrial damage and neurodegenerative diseases. *Neural Regen Res* 8(21):2003–2014. <https://doi.org/10.3969/j.issn.1673-5374.2013.21.009>
 78. Niizuma K, Endo H, Chan PH (2009) Oxidative stress and mitochondrial dysfunction as determinants of ischemic neuronal death and survival. *J Neurochem* 109(Supplement 1):133–138. <https://doi.org/10.1111/j.1471-4159.2009.05897.x>
 79. Lebre MC et al (2007) Human keratinocytes express functional toll-like receptor 3, 4, 5, and 9. *J Invest Dermatol* 127(2):331–341. <https://doi.org/10.1038/sj.jid.5700530>
 80. Lee CW et al (2016) Urban particulate matter down-regulates filaggrin via COX2 expression/PGE2 production leading to skin barrier dysfunction. *Sci Rep* 6:27995. <https://doi.org/10.1038/srep27995>
 81. Ryu YS et al (2019) Particulate matter induces inflammatory cytokine production via activation of NFκB by TLR5-NOX4-ROS signaling in human skin keratinocyte and mouse skin. *Redox Biol* 21:101080. <https://doi.org/10.1016/j.redox.2018.101080>
 82. Miao W et al (2005) Transcriptional regulation of NF-E2 p45-related factor (NRF2) expression by the aryl hydrocarbon receptor-xenobiotic response element signaling pathway: direct cross-talk between phase I and II drug-metabolizing enzymes. *J Biol Chem* 280(21):20340–20348. <https://doi.org/10.1074/jbc.M412081200>
 83. Köhle C, Bock KW (2007) Coordinate regulation of phase I and II xenobiotic metabolisms by the Ah receptor and Nrf2. *Biochem Pharmacol* 73(12):1853–1862. <https://doi.org/10.1016/j.bcp.2007.01.009>

Publisher's Note Springer Nature remains neutral with regard to jurisdictional claims in published maps and institutional affiliations.